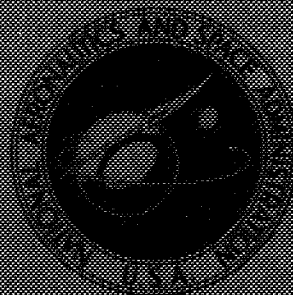


NASA TECHNICAL
MEMORANDUM



NASA TM X-3243

NASA TM X-3243

A METHOD FOR CALCULATING A REAL-GAS
TWO-DIMENSIONAL NOZZLE CONTOUR
INCLUDING THE EFFECTS OF GAMMA

Charles B. Johnson and Lillian R. Boney

Langley Research Center

Hampton, Va. 23665



NATIONAL AERONAUTICS AND SPACE ADMINISTRATION • WASHINGTON, D. C. • SEPTEMBER 1975

A METHOD FOR CALCULATING
A REAL-GAS TWO-DIMENSIONAL NOZZLE CONTOUR
INCLUDING THE EFFECTS OF GAMMA

Charles B. Johnson and Lillian R. Boney
Langley Research Center

SUMMARY

A method for calculating two-dimensional inviscid nozzle contours for a real gas or an ideal gas by the method of characteristics is described. The method consists of a modification of an existing nozzle computer program. The ideal-gas nozzle contour can be calculated for any constant value of gamma. Two new methods of calculating the center-line boundary values of the Mach number in the throat region are also presented. The use of these three methods of calculating the center-line Mach number distribution in the throat region can change the distance from the throat to the inflection point by a factor of 2.5.

The effect of ratios of specific heat (gamma) equal to 1.6667, 1.4, 1.25, and 1.1 on two-dimensional nozzle contours with constant area ratios and nearly constant lengths showed that a decrease in gamma resulted in a much more gradual opening of the nozzle contour from the throat into the expansion region. For similar area ratio and length constraints and for the same values of gamma, calculations of axisymmetric nozzle contours showed a trend similar to that of the two-dimensional nozzle contours; however, the effect of gamma on the axisymmetric contours was not nearly as pronounced as the effect on the two-dimensional contours. The effect of gammas of 1.6667, 1.4, 1.25, and 1.1 was investigated for two-dimensional and axisymmetric inviscid nozzle contours with a constant exit Mach number. The effect of decreasing the gamma in the calculation of the two-dimensional nozzle contour resulted in a more gradual opening of the nozzle from the throat into the expansion region. The effect on axisymmetric contours for calculations made with the same four values of gamma was similar to the effect found for the two-dimensional contours; however, the effect on the axisymmetric contours was not as pronounced as the effect on the two-dimensional contours. For the two-dimensional nozzle contours with a constant exit Mach number, the ratio of the exit height to throat height increased sharply with a decrease in the value of gamma. For a fixed throat size, the length of the two-dimensional nozzle decreased significantly with an increase in the value of gamma.

A user's guide is presented for input to the computer program for both the two-dimensional and axisymmetric nozzle contours.

INTRODUCTION

The calculation of supersonic and hypersonic nozzle contours by the method of characteristics has been used in the design of turbines, rockets, and wind tunnels. A review of many of the methods of supersonic nozzle calculation is given in reference 1, while additional methods are presented in references 2 to 9. This paper presents some of the major modifications made to an inviscid nozzle computer program since it was presented in reference 10. The modifications include a new technique of obtaining the starting center line and a method for calculating two-dimensional nozzle contours for a real gas or an ideal gas by using a modified version of the axisymmetric program presented in reference 10. In addition, a user's guide is given in order that the proper input can be used to select one of the 24 options that may be used in the calculation of an inviscid nozzle contour. Other input parameters used to form boundary conditions for the characteristic mesh are presented in the form of curves for ratios of specific heat (γ) of 1.6667, 1.4, 1.25, and 1.1. Sample nozzle contours are also presented for the above four values of γ and for parts of the nozzles which use a high temperature combustion gas. Portions of the nozzle contours calculated using the high temperature combustion products are presented for the maximum turning angles (θ_c) of 7.5° , 12° , 15° , 18° , and 20° and for the throat regions with three different center-line Mach number distributions.

SYMBOLS

A,B,C,D,E	coordinate points for starting nozzle calculations (cf. sketches (a) and (b))
\bar{A}	coefficient defined by equation (13)
A',B',C'	coefficients defined in equation (15)
a	velocity of sound
\bar{C},\bar{D}	coefficients defined in equation (1)
H_t	stagnation enthalpy
L	nondimensionalizing scale factor for nozzle contours
M	Mach number
p	pressure
r	distance measured from the source point in a radial flow field

r_{cr}	distance measured from the source point to a sonic sphere in radial flow
s	distance along a Mach line
u	velocity component in the x direction
u_l	limiting velocity
v	velocity component in the y direction
W	limiting velocity ratio, u/u_l
X_{inc}	incremental change in x distance defined by equation (14)
x	distance along nozzle plane of symmetry (or axis) with $x = 0$ at nozzle throat
y	distance measured perpendicular to nozzle plane of symmetry (or axis)
γ	ratio of specific heats
θ	flow angle, rad
θ_I	integrated values of flow angle as given by equation (A6)
θ_c	maximum turning angle, deg
μ	Mach angle, $\sin^{-1}\left(\frac{1}{M}\right)$
ρ	density
ψ	stream function
$\bar{\psi}$	nondimensional stream function

Subscripts:

A,B,C,D,E properties evaluated at points defined by sketches (a) and (b), with A referring to point evaluated at the nozzle throat

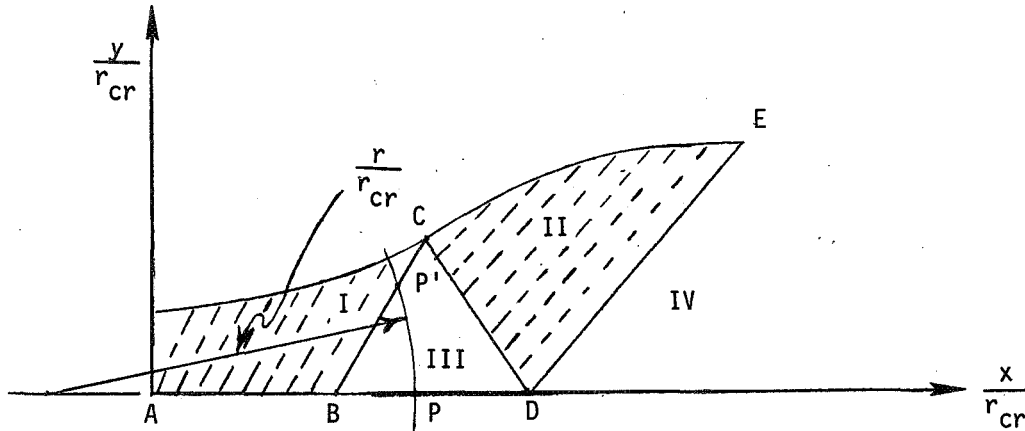
- lim value of the stream function that defines the inviscid nozzle contour
- t total conditions in the stagnation chamber
- ∞ free-stream uniform flow conditions

METHOD OF CALCULATION

Determination of Center-Line Mach Number Distribution

A detailed method of calculating axisymmetric inviscid nozzle contours was presented in reference 10. This method included a means of obtaining the boundary conditions for the construction of a characteristic mesh which used a linear Mach number distribution in the throat region. The method for obtaining the boundary conditions presented in this report is a modified version of the method presented in reference 10 and can be applied to the calculation of either two-dimensional or axisymmetric inviscid nozzle contours. In order to construct a characteristic mesh by the method of reference 10, the Mach number, the flow angle, and the value of the stream function must be known along the center line in the expansion region, along the radial-flow region boundaries, and along the final Mach line. The new method presented in this report starts the characteristic mesh at the final Mach line and calculates along Mach lines which start at the nozzle center line. The calculation ends at a point in the throat region where the Mach number is slightly greater than 1.0. On the center line the stream function and flow angle are zero and along the final Mach line the Mach number is constant, the flow angle is zero, and the stream function is easily calculated along the final Mach line as a function of the y coordinate. Thus, the only boundary condition to be determined is the Mach number distribution along the center line.

As presented in reference 10, the method of calculating the initial flow conditions for starting the characteristic mesh divided the inviscid nozzle flow into four regions as shown in sketch (a). The flow in region IV is a uniform parallel flow at the design Mach number of the nozzle. The triangular region III (BCD) is a radial-flow region which defines the flow along the boundaries B to C and C to D. In reference 10 a linear Mach number distribution is assumed from point A to B, where the Mach number is defined by the radial-flow region. The boundary from D to E is the final Mach line and has a constant Mach number and a 0° flow angle. Regions I and II use the flow properties on the boundaries A to B to C and C to D to E, respectively, to start the construction of the characteristic mesh. The calculation starts at point D and moves up the Mach line that is just upstream of the final Mach line (Mach lines of the first family shown by dashed lines in sketch (a)) until the integrated value of the stream function (along the Mach line) is reached. It can be seen from sketch (a) that as the calculation proceeds from point D to point C the

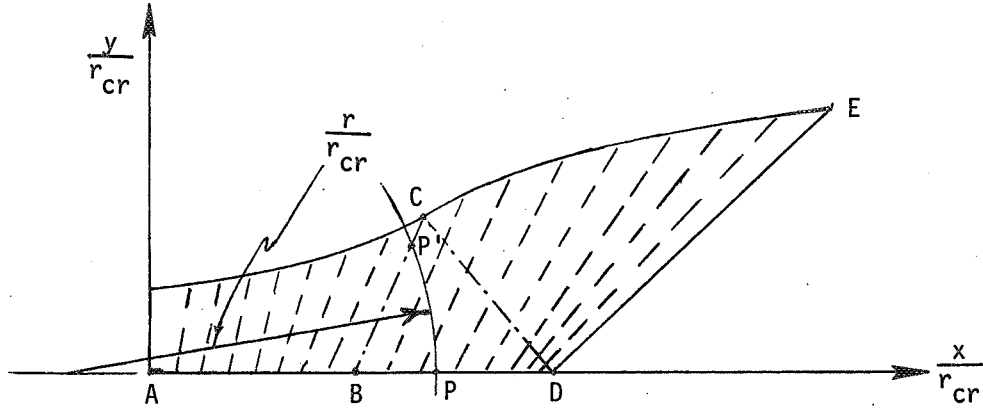


Sketch (a)

Mach lines (dash lines) decrease in length until just before point C is reached the Mach line is extremely short. After the Mach line closest to point C is constructed, the calculation returns to a Mach line just upstream of point B in region I. Sketch (a) indicates that the last Mach line calculated in region II is much shorter than the first Mach line calculated in region I.

These two different length Mach lines are used to calculate adjacent inviscid boundary (contour) points which are determined by a numerical integration of the stream function along the Mach lines. The numerical integration of the stream function along two different length Mach lines results in a discontinuity in the inviscid contour as demonstrated at the inflection point (point C) in figure 1. The discontinuity at point C is believed to result from a cumulative error in the numerical integration of the stream function, coupled with a small cumulative error inherent with a numerical finite-difference calculation with successive approximations. From figure 1 it should be noted that the error in the y ordinate caused by the discontinuity is less than 2 percent; however, this discontinuity can be removed by using a different method of obtaining the boundary condition for the characteristic mesh.

The discontinuity at the inflection point can be removed by starting all the mesh points (Mach lines) from the center line (points D to B to A) as shown in sketch (b). The center-line Mach number distribution from point D to point B is calculated using the same radial-flow equations used previously in sketch (a) along B to C and C to D. The center-line Mach number distribution is obtained by scribing an arc with a radius of r/r_{cr} from point P' down to point P on the center line (see sketches (a) and (b)) where the Mach number at point P' equals that at point P. Thus, the entire characteristic mesh can be started from the center line with Mach lines gradually decreasing in length, and the discontinuity at the inflection point found with the method of reference 10 can be avoided.



Sketch (b)

In reference 10 the method of determining the Mach number distribution from point A (nozzle minimum) to point B used a linear Mach number distribution. This linear distribution of Mach number from A to B produced a finite Mach number gradient with respect to axial distance at the throat. It was pointed out in reference 1 that in order to have a straight sonic line normal to the axis at the nozzle minimum, the Mach number gradient must be zero at the sonic point. It was also pointed out in reference 1 that experimental results have shown that the best flow is obtained when small maximum turning angles are used in conjunction with the requirement that $\frac{dM}{d\left(\frac{x}{r_{cr}}\right)} = 0$ at the throat; this requirement

results in a relatively long smooth contour that approaches zero curvature at the sonic point. Therefore, in order to improve the quality of the flow in the throat region the method of obtaining a Mach number distribution along the center line from point A to B was changed from a linear expression (ref. 10) to

$$M_{AtoB} = 1 + \bar{C}\left(\frac{x}{r_{cr}}\right)^2 + \bar{D}\left(\frac{x}{r_{cr}}\right)^3 \quad (\text{Referred to as } ABKEY = 1) \quad (1)$$

where

$$\bar{C} = \frac{1}{\left(\frac{x}{r_{cr}}\right)_B^2} \left\{ 3(M_B - 1) - \left(\frac{x}{r_{cr}}\right)_B \left[\frac{dM}{d\left(\frac{x}{r_{cr}}\right)} \right]_B \right\} \quad (2)$$

and

$$\bar{D} = \frac{1}{\left(\frac{x}{r_{cr}}\right)_B^3} \left\{ \left(\frac{x}{r_{cr}}\right)_B \left[\frac{dM}{d\left(\frac{x}{r_{cr}}\right)} \right]_B - 2(M_B - 1) \right\} \quad (3)$$

The boundary conditions at $\frac{x}{r_{cr}} = 0$ are

$$M = 1.0 \quad (4)$$

$$\frac{dM}{d\left(\frac{x}{r_{cr}}\right)} = 0 \quad (5)$$

and at $\frac{x}{r_{cr}} = \left(\frac{x}{r_{cr}}\right)_B$ they are

$$M = M_B \quad \left(\text{Evaluated at } \left(\frac{r}{r_{cr}}\right)_B\right) \quad (6)$$

$$\frac{dM}{d\left(\frac{x}{r_{cr}}\right)} = \left[\frac{dM}{d\left(\frac{r}{r_{cr}}\right)} \right]_B \quad \left(\text{Evaluated at } \left(\frac{r}{r_{cr}}\right)_B\right) \quad (7)$$

Equations (2) and (3) cannot be solved until a value for $\left(\frac{x}{r_{cr}}\right)_B$ is determined.

Between the two end points of the throat region $\left(\frac{x}{r_{cr}}\right)_A \leq \frac{x}{r_{cr}} \leq \left(\frac{x}{r_{cr}}\right)_B$, it is required that

$$\frac{dM}{d\left(\frac{x}{r_{cr}}\right)} \geq 0 \quad (8)$$

$$\frac{d^2M}{d\left(\frac{x}{r_{cr}}\right)^2} > 0 \quad (9)$$

The limitation given by equation (8) yields an increasing Mach number as $\frac{x}{r_{cr}}$ increases.

The condition of equation (9) gives a Mach number gradient which increases monotonically from a value of zero at the throat to a value of $\left[\frac{dM}{d\left(\frac{x}{r_{cr}}\right)} \right]_B$ at B.

The expressions for $\frac{dM}{d\left(\frac{x}{r_{cr}}\right)}$ and $\frac{d^2M}{d\left(\frac{x}{r_{cr}}\right)^2}$ from equation (1) are

$$\frac{dM}{d\left(\frac{x}{r_{cr}}\right)} = 2\bar{C}\left(\frac{x}{r_{cr}}\right) + 3\bar{D}\left(\frac{x}{r_{cr}}\right)^2 \quad (10)$$

$$\frac{d^2M}{d\left(\frac{x}{r_{cr}}\right)^2} = 2\bar{C} + 6\bar{D}\left(\frac{x}{r_{cr}}\right) \quad (11)$$

Equations (10) and (11) indicated that in order for the conditions of equations (8) and (9) to be satisfied, that \bar{C} and \bar{D} must be greater than zero. Positive values of \bar{C} and \bar{D} are assured if a parameter found from the terms in equations (2) and (3) has the following limits

$$2 < \frac{\left(\frac{x}{r_{cr}}\right)_B \left[\frac{dM}{d\left(\frac{r}{r_{cr}}\right)} \right]_B}{M_B - 1} < 3 \quad (12)$$

Equation (12) implies that the value of $\left(\frac{x}{r_{cr}}\right)_B$ is found from

$$\left(\frac{x}{r_{cr}}\right)_B = \bar{A} \frac{M_B - 1}{\left[\frac{dM}{d\left(\frac{r}{r_{cr}}\right)} \right]_B} \quad (13)$$

where \bar{A} is an arbitrary constant that must be an input into the computer program and that must have a value between 2.0 and 3.0. Thus, with the value of $\left(\frac{x}{r_{cr}}\right)_B$ from equation (13), equations (1), (2), and (3) may be solved. The values of M_B and $\left[\frac{dM}{d\left(\frac{r}{r_{cr}}\right)} \right]_B$ are determined from the radial-flow calculations. If $\bar{A} = 1.0$ is used in equation (13), the value of $\left(\frac{x}{r_{cr}}\right)_B$ is the same as that found for a linear Mach number distribution from A to B.

After the value of $\left(\frac{x}{r_{cr}}\right)_B$ is determined the Mach number distribution from point A to B is found from equation (1). The values of $\frac{r}{r_{cr}}$ from point B to D are changed to $\frac{x}{r_{cr}}$ values by adding X_{inc} to the $\frac{r}{r_{cr}}$ values, where

$$X_{inc} = \left(\frac{x}{r_{cr}}\right)_B - \left(\frac{r}{r_{cr}}\right)_B \quad (14)$$

Two methods of calculating a center-line Mach number distribution from A to B (see sketch (a)) have been described. The first method stipulated a linear Mach number distribution from A to B with a finite slope of $\left[\frac{dM}{d\left(\frac{r}{r_{cr}}\right)} \right]_B$ at $\frac{x}{r_{cr}} = 0$. The second method used a third order polynomial (eq. (1)) to describe the distribution of Mach number as a

function of $\frac{x}{r_{cr}}$. The boundary conditions stipulated that $\frac{dM}{d\left(\frac{x}{r_{cr}}\right)} = 0$ at $\frac{x}{r_{cr}} = 0$. The use of the second method resulted in a throat region that was two to three times longer than the region calculated from the linear variation of Mach number.

If the nozzle design requires a shorter throat region from A to B than can be calculated using a linear Mach number distribution, a third method for finding the Mach number distribution from A to B can be used. The third method used a second order polynomial given by

$$M = A' + B'\left(\frac{x}{r_{cr}}\right) + C'\left(\frac{x}{r_{cr}}\right)^2 \quad (\text{Referred to as ABKEY} = -1) \quad (15)$$

where

$$A' = 1.0 \quad (16)$$

$$B' = \left[\frac{dM}{d\left(\frac{x}{r_{cr}}\right)} \right]_A \quad (17)$$

$$C' = \frac{\left[\frac{dM}{d\left(\frac{x}{r_{cr}}\right)} \right]_B^2 - \left[\frac{dM}{d\left(\frac{x}{r_{cr}}\right)} \right]_A^2}{4(M_B - 1)} \quad (18)$$

The boundary conditions are:

At

$$\frac{x}{r_{cr}} = \left(\frac{x}{r_{cr}}\right)_A = 0$$

$$M = 1.0$$

$$\left[\frac{dM}{d\left(\frac{x}{r_{cr}}\right)} \right]_A > \left[\frac{dM}{d\left(\frac{x}{r_{cr}}\right)} \right]_B$$

and at $\frac{x}{r_{cr}} = \left(\frac{x}{r_{cr}}\right)_B$ are

$$M = M_B$$

$$\left[\frac{dM}{d\left(\frac{x}{r_{cr}}\right)} \right]_B = \left[\frac{dM}{d\left(\frac{x}{r_{cr}}\right)} \right]_B$$

The value of $\left(\frac{x}{r_{cr}}\right)_B$ is found from

$$\left(\frac{x}{r_{cr}}\right)_B = \frac{2(M_B - 1)}{\left[\frac{dM}{d\left(\frac{x}{r_{cr}}\right)}\right]_A + \left[\frac{dM}{d\left(\frac{r}{r_{cr}}\right)}\right]_B} \quad (19)$$

The stipulation in the use of equation (16) is that any finite value of $\left[\frac{dM}{d\left(\frac{x}{r_{cr}}\right)}\right]_A$ that is used must be larger than $\left[\frac{dM}{d\left(\frac{r}{r_{cr}}\right)}\right]_B$. The value of $\left[\frac{dM}{d\left(\frac{x}{r_{cr}}\right)}\right]_A$, used in equation (19), gives a value of $\left(\frac{x}{r_{cr}}\right)_B$ that is smaller than the value found from the previously discussed method and also smaller in value than the method of reference 10 (i.e., linear Mach number distribution). When the slopes at points A and B are equal, equation (19) reduces to the linear Mach number distribution of reference 10. When $\left[\frac{dM}{d\left(\frac{r}{r_{cr}}\right)}\right]_A$ is two or three times greater than $\left[\frac{dM}{d\left(\frac{r}{r_{cr}}\right)}\right]_B$, the $\left(\frac{x}{r_{cr}}\right)_B$ is two-thirds or one-half, respectively, of the $\left(\frac{x}{r_{cr}}\right)_B$ distance found using the linear Mach number distribution from A to B.

After the value of $\left(\frac{x}{r_{cr}}\right)_B$ is determined, equations (15) to (18) are solved for the Mach number distribution along the center line from A to B. The values of $\frac{r}{r_{cr}}$ between point B and D (including point D) are changed to $\frac{x}{r_{cr}}$ values by adding X_{inc} to the $\frac{r}{r_{cr}}$ values using equation (14).

RESULTS AND DISCUSSION

Two-Dimensional Nozzle Calculations

The design of a two-dimensional real-gas nozzle contour was required as part of the design of a thermal protection system test facility at the Langley Research Center; this facility burns a mixture of air, oxygen, and methane in a settling chamber and expands the products of combustion in the nozzle. These products of combustion have an effective value of gamma of approximately 1.25. The method used for calculating two-dimensional nozzle contours is given in the appendix. The combustion facility will be used to test space shuttle panels under the conditions of heating expected in flight. The mechanical design criteria necessitated that the nozzle have as short a length as possible (to avoid

excessive heat transfer) within the limits of the two-dimensional method of calculation described in this report. In order to assess the effect of the maximum turning angle on the length of the nozzle, real-gas inviscid nozzle contours were calculated for maximum turning angles of 7.5° , 12° , 15° , 18° , and 20° and are shown in figure 2. The nozzle contours were calculated with a linear Mach number distribution on the center line of the expansion region (A to B, sketch (b)) and for a real-gas Mach number of 3.777. The Mach number was selected from the real-gas flow properties at a stagnation pressure and enthalpy of 10 atm and 5.307×10^6 joules/kg in order to give an inviscid area ratio of 25. The results in figure 2 showed that as the maximum flow angle increases the length of the nozzle decreases. For instance, an increase in the maximum flow angle from 7.5° to 15° reduces the length of the nozzle to slightly half the original length.

The nozzle can also be shortened by selecting the Mach number distribution along the center line (A to B, sketch (b)); the ABKEY = -1 gives the shortest expansion region. Figure 3 illustrates the effect of using the three different center-line Mach number distributions; where ABKEY = 1 is the distribution given by equation (1), ABKEY = 0 is the linear distribution used in reference 10, and ABKEY = -1 is the distribution given by equation (15). The nozzle calculations in figure 3 were made for a combustion facility using real-gas flow properties, with a design Mach number of 3.777. The expansion region with $\frac{dM}{d\left(\frac{x}{L}\right)} = 0$ at the throat (ABKEY = 1) has the greatest distance from the throat to the inflection point C $\left(\left(\frac{x}{L}\right)_C \approx 51\right)$. The linear distribution (ABKEY = 0) shortens the distance from the throat to the inflection point to almost half the distance calculated by the ABKEY = 1 method. The use of the ABKEY = -1 method compared to the ABKEY = 1 method reduces the length of the nozzle from the throat to the inflection point by a factor of approximately 2.5. Ideally, a nozzle should have a zero Mach number gradient at the throat as given by the ABKEY = 1 design. However, the very gradual opening of the throat region of the nozzle using the ABKEY = 1, as seen in figure 3, presents design and fabrication problems as well as an excessive heat load to the nozzle. Problems such as these dictate that the ABKEY = -1 design method should be used for a nozzle that operates at high enthalpy stagnation conditions. The combustion products have an effective gamma of approximately 1.25 which coupled with the ABKEY = 1 method of calculating the throat region results in a gradual opening of the throat region as previously noted in figure 3. The very gradual opening of the throat region for the ABKEY = 1 method would be accentuated in the design of nozzle contours for a gas that has a gamma of approximately 1.1 (similar to tetrafluoromethane (CF_4)). Thus, for nozzles with small values of effective gammas (i.e., $\gamma \approx 1.1$), both the maximum turning angle and the type of throat region must be carefully chosen to satisfy certain mechanical and heat transfer design criteria.

The Effect of Gamma On Nozzle Contours

The results in figure 3 indicated that for a gamma of approximately 1.25 the nozzle had a very gradual opening in the expansion region. In order to study the effect of gamma on nozzle contours, two-dimensional calculations were made for gammas of 1.6667, 1.4, 1.25, and 1.1, these gammas represent the value of gamma for helium, ideal-gas air, combustion products (or high temperature air), and tetrafluoromethane, respectively, and are shown in figure 4. The calculations were made for a constant value of gamma using ideal-gas expressions. The four contours were calculated for a constant throat-to-exit area ratio of 25 and a constant maximum turning angle of 12° . In order to get a constant area ratio for the four values of gamma, the design Mach number was varied from 7.11 to 3.49 from the highest to lowest value of gamma, respectively. In addition to the constant area ratio, the four contours had the same total length at an x/L value of about 64. For two-dimensional nozzles of a given area ratio and given length, the effect of decreasing gamma (see fig. 4) results in a more gradual opening of the nozzle from the throat into the expansion region.

A comparison of four axisymmetric nozzle contours calculated for gammas of 1.6667, 1.4, 1.25, and 1.1 is shown in figure 5. The comparison in figure 5 is for the same values of gamma, the same Mach numbers, and the same constant area ratio as was used in figure 4. The effect of gamma on the axisymmetric nozzle contours is similar to the effect found in figure 4; for example, there is a more gradual opening of the expansion region as the value of gamma decreases. However, for the axisymmetric contours in figure 5, the variation in the expansion region is not as pronounced as was found for the two-dimensional contours in figure 4.

Two-dimensional nozzle contours calculated at a constant exit Mach number of 5.0 for values of gamma of 1.6667, 1.4, 1.25, and 1.1 are shown in figure 6. The four nozzle contours had a fixed throat size ($\frac{y}{L} = 0.24$) for the purpose of facilitating a comparison of the effect of gamma on the contours. The nozzle contour in the expansion region just downstream of the throat begins to open more rapidly as the value of gamma increases from 1.1 to 1.6667. The area ratios for the four contours have values of 597.7, 69.22, 25.00, and 9.804 for values of gamma of 1.1, 1.25, 1.4, and 1.6667, respectively. For two-dimensional nozzles, the variation in area ratio is accentuated because the area ratio varies directly as the ratio of the exit height to the throat height. Thus, for a fixed throat size the nozzle calculated for $\gamma = 1.1$ is large relative to the nozzle calculated for $\gamma = 1.6667$. The ratio of nozzle lengths for the nozzle designed for $\gamma = 1.1$ to the one designed for $\gamma = 1.6667$ is approximately 80.

Axisymmetric nozzle contours calculated for values of gamma of 1.6667, 1.4, 1.25, and 1.1 and for a constant exit Mach number of 5.0 are shown in figure 7. Again, the four contours had the same throat radius ($\frac{y}{L} = 0.24$, i.e., the same throat height as that used

for the two-dimensional contours in fig. 6) for the purpose of facilitating a comparison of the effect of gamma on the contours. Similar to the two-dimensional contours, the contour in the expansion region begins to open more rapidly as the value of gamma increases from 1.1 to 1.6667. The area ratios for the four contours are the same for the respective values of gamma as the two-dimensional nozzles in figure 6. However, the variation in exit radius for the axisymmetric nozzles is not as great as that for the two-dimensional nozzles. For the axisymmetric contours, for a given area ratio, the variation in exit radius varies as the square of the radius. Thus, the variation in exit radius is much less for the axisymmetric nozzles than it is for the two-dimensional nozzles. The ratio of nozzle lengths for an axisymmetric nozzle designed for $\gamma = 1.1$ to the one designed for $\gamma = 1.6667$ is a factor of approximately 11 compared to the factor of approximately 80 found for the two-dimensional nozzle contours. Again, for a fixed throat radius, as was found for the two-dimensional contours, the size of the nozzle for $\gamma = 1.1$ is much larger than the nozzle calculated for $\gamma = 1.6667$.

CONCLUDING REMARKS

A method for calculating two-dimensional inviscid nozzle contours for an ideal or real gas is described. The method of calculation is similar to a previously reported method for calculating axisymmetric nozzle contours. A modified version of a previous method for obtaining the boundary conditions for starting the characteristic mesh of both the two-dimensional and axisymmetric inviscid contours is presented. In addition, two other methods of obtaining the Mach number distribution in the throat expansion region are presented. If required, the program can print out the entire flow-field properties as determined by a solution of the characteristic mesh. Normally the program just prints the inviscid nozzle coordinates with the flow properties (necessary for a boundary-layer calculation) given at the edge of an inviscid contour.

Calculations were made to minimize the length of a two-dimensional real-gas inviscid nozzle contour to be used in the design of a combustion facility that would test space shuttle panels. A variation of the maximum turning angle for two-dimensional nozzles showed that an increase in the flow angle from 7.5° to 15° reduced the length of the nozzle by approximately a factor of 2. The two new methods (designated ABKEY = -1 and ABKEY = 1) of determining the center-line Mach number distribution in the throat expansion region gave different center-line lengths from the throat to the inflection point. One of the methods shortens the nozzle (ABKEY = -1) whereas the other method (ABKEY = 1) gives a longer expansion region and also gives the proper boundary conditions for a straight sonic line perpendicular to the nozzle axis. The ABKEY = -1 (short-throat expansion region) method shortens the center-line distance from the throat to the inflection point by a factor of 2.5 compared to the ABKEY = 1 method (long-throat expansion).

The effect of ratios of specific heats (γ) of 1.6667, 1.4, 1.25, and 1.1 was investigated for two-dimensional and axisymmetric inviscid nozzle contours with variable exit Mach numbers, constant area ratios, and constant lengths between the throat and the exit. The effect of decreasing the γ in the calculation of the two-dimensional nozzle contours results in a more gradual opening of the nozzle from the throat into the expansion region. The effect on axisymmetric contours for calculations made with the same four values of γ was similar to the effect found for the two-dimensional contours; however, this effect on the axisymmetric contours was not as pronounced as that on the two-dimensional contours.

Two-dimensional nozzle contours which were calculated for γ s of 1.6667, 1.4, 1.25, and 1.1 with a constant exit Mach number, showed that a decrease in γ resulted in a much more gradual opening of the nozzle contour in the area of the expansion region. For the contours with a constant exit Mach number the ratio of the exit height to throat height increased sharply with a decrease in γ . For a fixed throat size the length of the two-dimensional nozzle decreased significantly with an increase in the value of γ . Axisymmetric nozzle contours, calculated with a constant exit Mach number and for the same four values of γ , showed that a decrease in γ gave a more gradual opening of the nozzle contour in the expansion region. This trend was similar to the two-dimensional nozzle contours; however, for the axisymmetric nozzle contours it was not nearly as pronounced.

A user's guide is presented in order to input the various options for two-dimensional and axisymmetric inviscid contours.

Langley Research Center
National Aeronautics and Space Administration
Hampton, Va. 23665
June 6, 1975

APPENDIX

ANALYSIS FOR CALCULATING TWO-DIMENSIONAL INVISCID NOZZLE CONTOURS

Characteristic Equations

The procedure for calculating an axisymmetric inviscid nozzle contour for a real gas is described in reference 10. The method of calculation used for the two-dimensional (2D) inviscid nozzle contour is very much the same as the method described in reference 10. The new technique of obtaining the center-line Mach number distribution and the three throat regions, both of which have been previously described in this report, are incorporated into both the two-dimensional method described herein and the axisymmetric method of calculation described in reference 10. The method of calculation allows for a complete description of the flow field as defined by the characteristic mesh and if required the entire flow-field properties can be printed by the program.

The assumption of a steady, irrotational flow results in the basic continuity and Euler's equations given as (see ref. 3, p. 19):

$$\frac{\partial(\rho u)}{\partial x} + \frac{\partial(\rho v)}{\partial y} = 0 \tag{A1}$$

$$\left. \begin{aligned} u \frac{\partial u}{\partial x} + v \frac{\partial u}{\partial y} &= -\frac{1}{\rho} \frac{\partial p}{\partial x} \\ u \frac{\partial v}{\partial x} + v \frac{\partial v}{\partial y} &= -\frac{1}{\rho} \frac{\partial p}{\partial y} \end{aligned} \right\} \tag{A2}$$

From equations (A1) and (A2) the two-dimensional characteristics equations are derived in the form (see ref. 3, ch. 2):

$$\left. \begin{aligned} \frac{dy}{dx} &= \tan(\theta + \mu) \\ \frac{dW}{W} - \tan \mu d\theta &= 0 \end{aligned} \right\} \text{First family} \tag{A3}$$

$$\left. \begin{aligned} \frac{dy}{dx} &= \tan(\theta - \mu) \\ \frac{dW}{W} + \tan \mu d\theta &= 0 \end{aligned} \right\} \text{Second family} \tag{A4}$$

APPENDIX

The characteristic equations are then written in a difference form and solved in a stepwise procedure by 3-point successive approximation. Further details are given in appendix A of reference 10.

Flow Properties Along Flow-Region Boundaries

As previously discussed in this report and in reference 10, the boundary conditions along the center line (A to D) and along the final Mach line (D to E) are required to start the characteristic mesh. (See sketch (a).) The region on the center line from B to D is determined by radial flow. Two-dimensional radial or source flow is defined as a flow in which all the flow properties are a function only of the distance r from a fixed point in the two-dimensional plane. The general equation for two-dimensional radial flow derived from "one-dimension gas dynamics" is

$$(M^2 - 1) \frac{dW}{W} - \frac{dr}{r} = 0 \quad (A5)$$

For the radial-flow region the equations for the integrated total expansion angle θ_I and the integrated distance $\frac{r}{r_c}$, as taken from equations (A3) and (A5), respectively, are

$$\theta_I = \int_{W(M=1.0)}^W \frac{\sqrt{M^2 - 1}}{W} dW \quad (A6)$$

$$\ln \frac{r}{r_c} = \int_{W(M=1)}^W \frac{M^2 - 1}{W} dW \quad (A7)$$

Calculation of Streamline Along an Inviscid Boundary

The fact that the boundary for the characteristic mesh no longer goes from B to C and from C to D (see ref. 10) does not mean that point C does not exist. Point C is still the inflection point on the inviscid boundary where the flow has its maximum turning angle. Also, as a carryover from the method described in reference 10, point C is where the radial-flow stream function $\bar{\psi}$ is evaluated in order to establish the limiting value $\bar{\psi}_{lim}$. The value of $\bar{\psi}_{lim}$ is used to determine the inviscid edge point on the first-family characteristic. The differential form of the two-dimensional radial-flow equation is

$$d\psi = \rho u r d\theta \quad (A8)$$

It is convenient to define a nondimensional stream function as

$$\bar{\psi} = \frac{\psi}{\rho_t u_t r_{cr}^2} \quad (A9)$$

APPENDIX

The resulting expression for the radial-flow stream function evaluated at point C is

$$\bar{\psi}_{\text{lim}} = \left(\frac{\rho}{\rho_t} \frac{u}{u_t} \frac{r}{r_{\text{cr}}} \theta \right)_C \quad (\text{A10})$$

The general differential form of the stream function for two-dimensional flow is

$$d\psi = \rho a ds \quad (\text{A11})$$

where a is the local speed of sound, and ds is the differential distance along a Mach line. When equations (A9) and (A11) are combined, the nondimensional form of the stream function is given by

$$\bar{\psi} = \int_0^{(s/r_{\text{cr}})} \frac{\rho}{\rho_t} W \sin \mu d\left(\frac{s}{r_{\text{cr}}}\right) \quad (\text{A12})$$

The value of $\bar{\psi}$ is calculated at each point along the first-family characteristic until a value which exceeds $\bar{\psi}_{\text{lim}}$ is reached. The flow properties and coordinates along the edge of inviscid contour are determined by interpolation between the $\bar{\psi}$ values which bound $\bar{\psi}_{\text{lim}}$. In the preliminary design of a two-dimensional or axisymmetric nozzle contour, it is convenient to know the integrated value of the flow angle θ_I and the value of $\frac{r}{r_{\text{cr}}}$ over the boundaries of the radial-flow region. (See sketches (a) and (b).) The values of θ_I and $\frac{r}{r_{\text{cr}}}$ as a function of Mach number for gammas of 1.1, 1.25, 1.4, and 1.6667 are shown in figures 8 and 9 for two-dimensional radial flow and in figures 10 and 11 for three-dimensional radial flow. The expressions for θ_I and $\frac{r}{r_{\text{cr}}}$ for two-dimensional flow are given in equations (A6) and (A7), respectively, and the two expressions for axisymmetric flow are given in reference 10. The curves in figure 8 or 10 may be used to obtain an estimate of the nozzle length for a given maximum turning angle θ_c and a given design Mach number. The value of $\theta_{I,B}$ and $\theta_{I,C}$ can be found from

$$\theta_{I,B} = \theta_{I,D} - 2\theta_C$$

$$\theta_{I,C} = \theta_{I,D} - \theta_C$$

where $\theta_{I,D}$ is evaluated at the design Mach number. The Mach numbers at point B and C can be found with $\theta_{I,B}$ and $\theta_{I,C}$ from figure 8 or 10. From the values of the Mach number at point B and C an assessment can be made of the Mach number distribution in the expansion region. The length of the nozzle can be determined by first evaluating $\bar{\psi}_{\text{lim}}$ at point C from equation (A10), then setting $\bar{\psi}$ of equation (A12) equal to $\bar{\psi}_{\text{lim}}$ and solving equation (A12) for $\frac{s}{r_{\text{cr}}}$ at sonic (nozzle-throat) conditions. The value of $\frac{s}{r_{\text{cr}}}$ at the throat is used to obtain a scale factor for the desired throat size. The scale factor is then used to convert $\left(\frac{r}{r_{\text{cr}}}\right)_D$ from figure 9 or 11 to a physical dimension which is approximately the distance from the nozzle throat to point D; i.e., the point on the nozzle center line where the final Mach line originates.

APPENDIX

Program Input Format

- \$N1** Card 1, starting in column 2.
- DOPT** 2 for two-dimensional contour.
3 for axisymmetric contour.
- GOPT** 1 for equations for gas properties; i.e., $\frac{1}{W^2} = 1 + \frac{2}{\gamma - 1} \left(\frac{1}{M^2} \right)$, $\frac{\rho}{\rho_t} = (1 - W^2)^{\frac{1}{\gamma - 1}}$,
and $\frac{p}{p_t} = (1 - W^2)^{\frac{\gamma}{\gamma - 1}}$
2 for gas tables of $1/W^2$, $1/M^2$, ρ/ρ_t , and p/p_t .
- GAM** Value of γ if GOPT = 1.
0 if GOPT = 2.
- CLINE** 1 if center-line Mach number distribution input on \$N2 cards.
0 if radial-flow equations are used to determine center-line Mach number distribution.
- EMTAB** Table of $1/M^2$, increasing values, limit of 200. Omit if GOPT = 1.
- WTAB** Table of $1/W^2$, increasing values, limit of 200. Omit if GOPT = 1.
- RHORT** Table of ρ/ρ_t , increasing values, limit of 200. Omit if GOPT = 1.
- PPG** Table of p/p_t , increasing values, limit of 200. Omit if GOPT = 1.
- N** Number of values in a gas table; i.e., number of values in $1/M^2$ table.
Omit if GOPT = 1.
- THETC** Maximum turning angle at point C, in radians. Omit if CLINE = 1.
- EMD** Design Mach number, value at point D. Omit if CLINE = 1.
- ABAR** Value of \bar{A} used with ABKEY = 1 for calculation $\left(\frac{x}{r_{cr}} \right)_B$ (eq. (13)).

APPENDIX

- ABKEY** -1 for shortest throat expansion region (requires value of DMDXA).
 0 for linear center-line Mach number distribution in the throat expansion
 region.
 1 for longest throat expansion region (third order polynomial for Mach number
 distribution of the center line).
 Omit if $CLINE = 1$.
- DMDXA** Value of $\frac{dM}{d\left(\frac{x}{r_{cr}}\right)}$ at point A (throat). If $ABKEY = -1$, omit if $CLINE = 1$.
- DELW** The integration interval (dW) for the radial-flow equations (eqs. (A6) and (A7)
 and ref. 10). Omit if $CLINE = 1$.
- RLIM** The value of r/r_{cr} above which the r/r_{cr} spacing $(\Delta r/r_{cr})$ is kept within
 a limit defined by DRORCR. (This must be determined from an initial trial
 calculation of the radial-flow region.) Omit if $CLINE = 1$.
- DRORCR** Limit on the r/r_{cr} spacing $(\Delta r/r_{cr})$ after RLIM is reached. Omit if
 $CLINE = 1$.
- RERR** Error limit on the value of DRORCR. Omit if $CLINE = 1$.
- DDW** Change in DELW required to keep DRORCR within the error limit RERR.
 Omit if $CLINE = 1$.
- DXDE** Delta $\frac{x}{r_{cr}}$ along DE. Omit if $CLINE = 1$.
- NABB** Number of points from A to B. Omit if $CLINE = 1$.
- MAX** The maximum number of boundary points on the center line and the final Mach
 line, set at 1500. Omit if $CLINE = 1$.
- \$** Start in column 2.
- For $CLINE = 1$:
- \$N2** Start in column 2.
- XC** $\frac{x}{r_{cr}}$ value on the center line at the origin of the final Mach line. Omit if
 $CLINE = 0$.

APPENDIX

- EMC Mach number along the final Mach line originating at XC. Omit if CLINE = 0.
- DXBC The $\frac{x}{r_{cr}}$ increment along the final Mach line. Omit if CLINE = 0.
- PSID Value of stream function used to define inviscid contour. Omit if CLINE = 0.
- \$ In column 2.

For the CLINE = 1 option each point on the center line from the point just upstream of the final Mach line to throat must have a value of XC and EMC on a card with the following format:

- \$N2 Column 2.
- XC Point on the center line.
- EMC Mach number corresponding to XC.
- \$ Column 2.

After the center-line Mach number distribution has been input a final card is input:

- \$N2 Column 2.
- XC A value of 0.
- EMC A value of 0.
- \$ Column 2.

The next set of inputs are:

- \$N1 Column 2.
- NAPRX Set equal to 3. It is the number of approximations used in the solution of the characteristic mesh points.
- PRINT 1 print characteristic network.
0 print inviscid wall points only.

APPENDIX

AREA 1 starts case.

NN Number of values in table of $1/M^2$. Omit if GOPT = 1.

\$ Column 2.

The final card is:

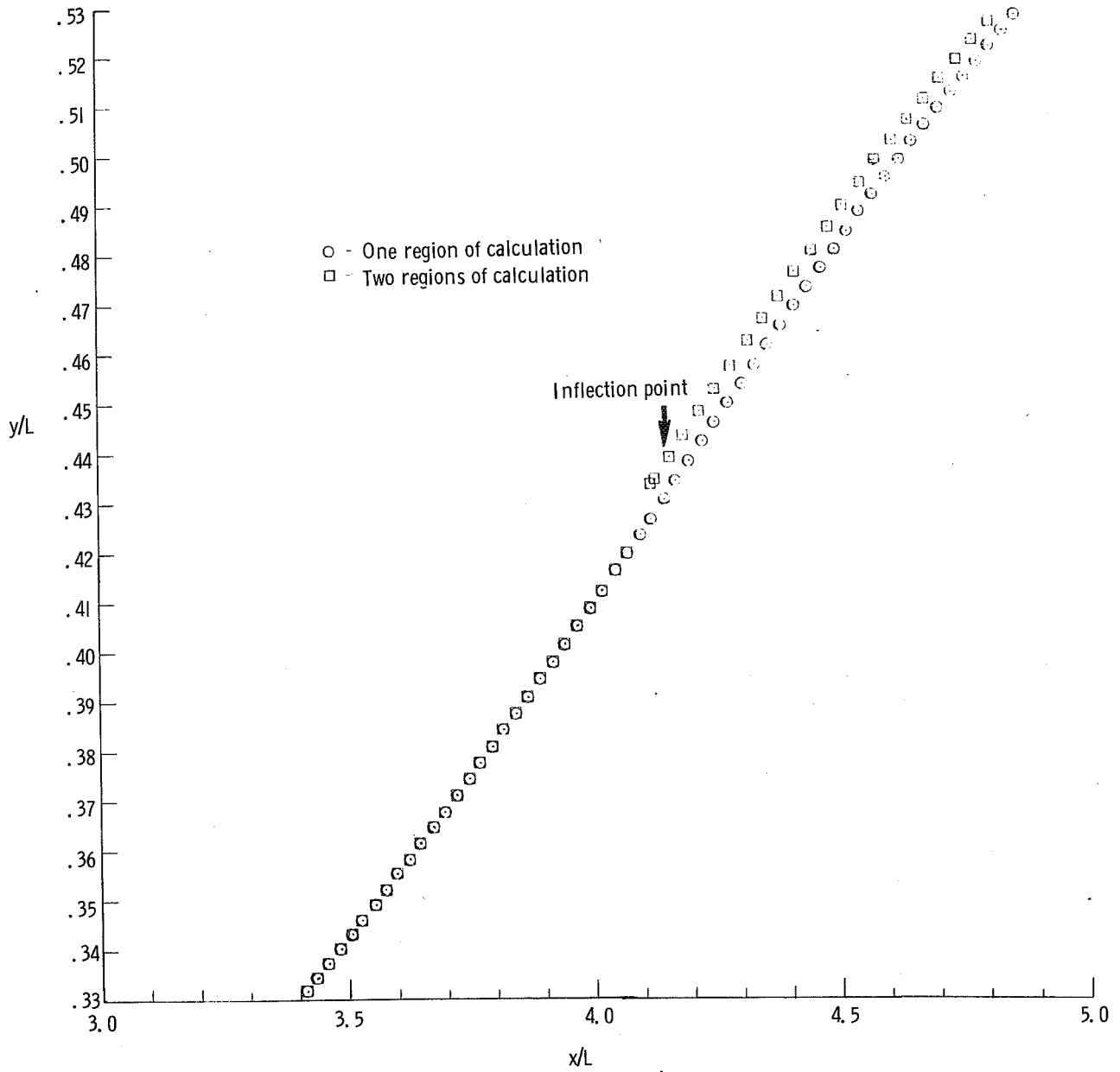
\$N1 Column 2.

AREA 2 ends case.

\$ Column 2.

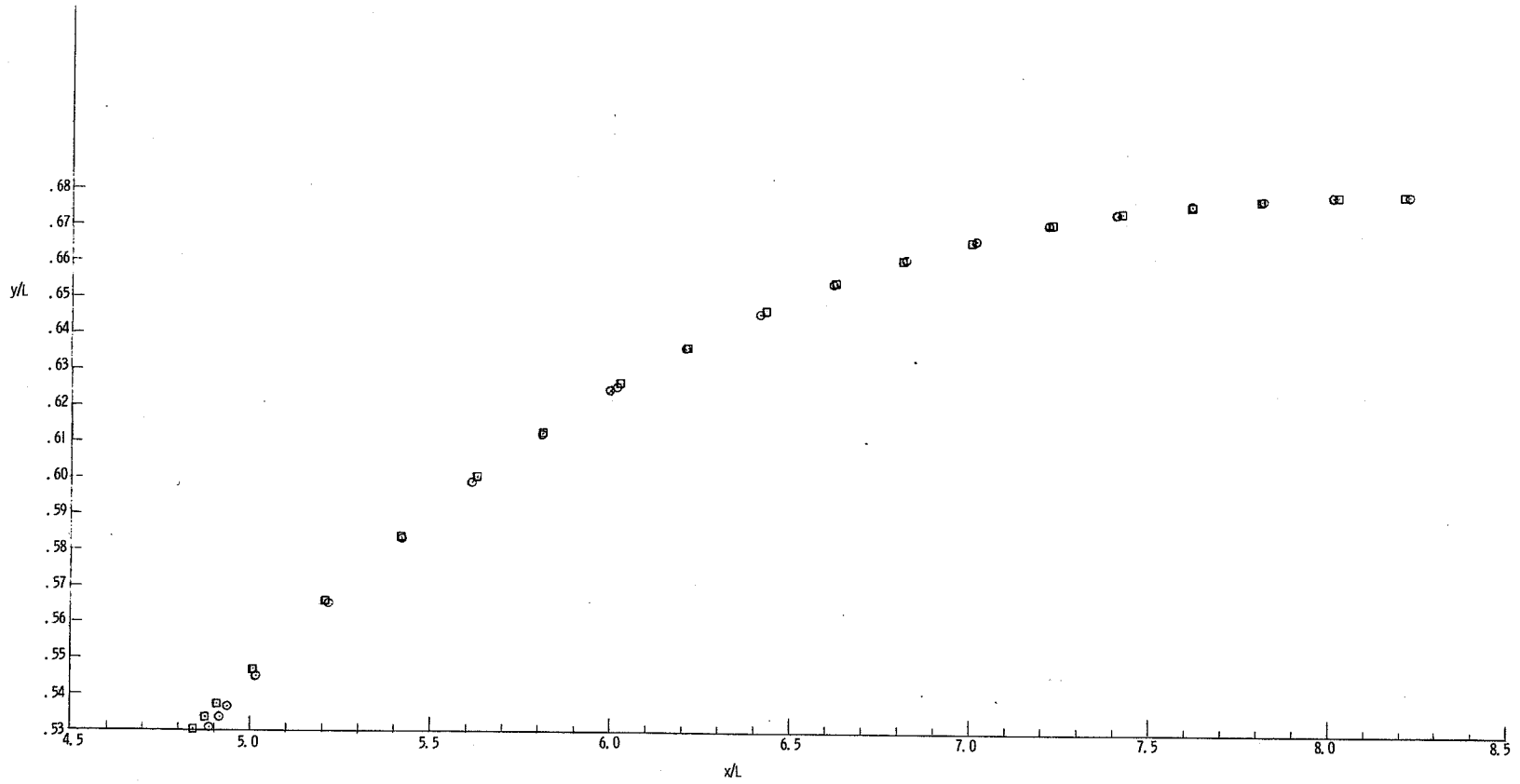
REFERENCES

1. McCabe, A.: Design of a Supersonic Nozzle. R & M, No. 3440, British A.R.C., 1967.
2. Beckwith, Ivan E.; and Moore, John A.: An Accurate and Rapid Method for the Design of Supersonic Nozzles. NACA TN 3322, 1955.
3. Ferri, Antonio: Elements of Aerodynamics of Supersonic Flows. MacMillan Co., 1949.
4. Beckwith, Ivan E.; Ridyard, Herbert W.; and Cromer, Nancy: The Aerodynamic Design of High Mach Number Nozzles Utilizing Axisymmetric Flow With Application to a Nozzle of Square Test Section. NACA TN 2711, 1952.
5. Guentert, Eleanor Costilow; and Neumann, Harvey E.: Design of Axisymmetric Exhaust Nozzles by Method of Characteristics Incorporating a Variable Isentropic Exponent. NASA TR R-33, 1959.
6. Enkenhus, K. R.; and Maher, E. F.: The Aerodynamic Design of Axisymmetric Nozzles for High-Temperature Air. NAVWEPS Rep. 7395, U.S. Navy, Feb. 5, 1962.
7. Erickson, Wayne D.; and Creekmore, Helen S.: A Study of Equilibrium Real-Gas Effects in Hypersonic Air Nozzles, Including Charts of Thermodynamic Properties for Equilibrium Air. NASA TN D-231, 1960.
8. Glowacki, Walter J.: NOL Hypervelocity Wind Tunnel Report No. 2: Nozzle Design. NOLTR 71-6, U.S. Navy, Apr. 30, 1971.
9. Vanco, Michael R.; and Goldman, Louis J.: Computer Program for Design of Two-Dimensional Supersonic Nozzle With Sharp-Edged Throat. NASA TM X-1502, 1968.
10. Johnson, Charles B.; Boney, Lillian R.; Ellison, James C.; and Erickson, Wayne D.: Real-Gas Effects on Hypersonic Nozzle Contours With a Method of Calculation. NASA TN D-1622, 1963.



(a) End of expansion region, including inflection point and start of turning region.

Figure 1.- A comparison of two-region method of calculation with the one region of method of calculation for an inviscid nozzle contour.



(b) End of turning region to nozzle exit.

Figure 1.- Concluded.

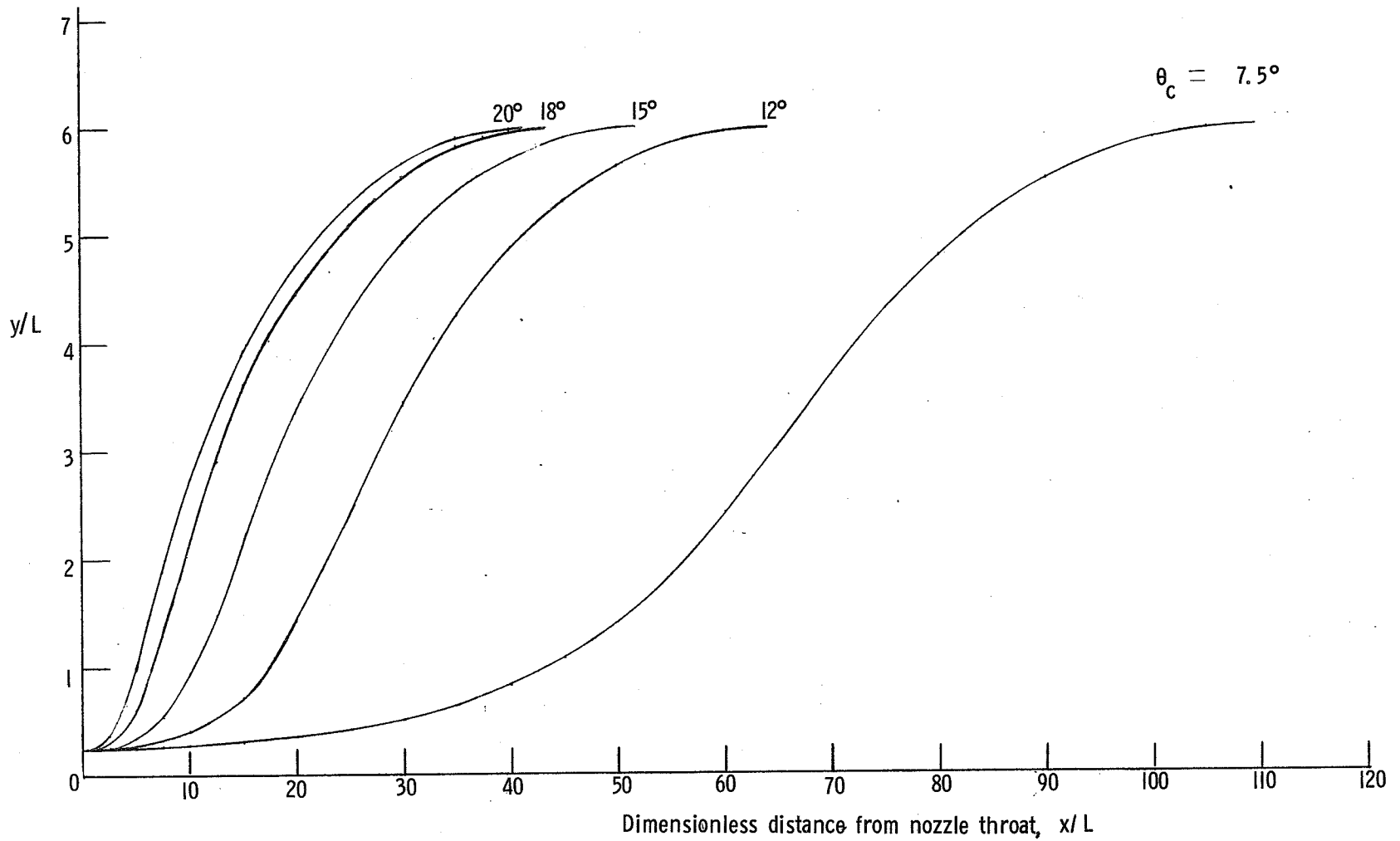


Figure 2.- The effect of various maximum turning angles on two-dimensional real-gas nozzle contours (ABKEY = 0), ($p_t = 10$ atm, $H_t = 5.307 \times 10^6$ joules/kg), and ($\gamma \approx 1.25$).

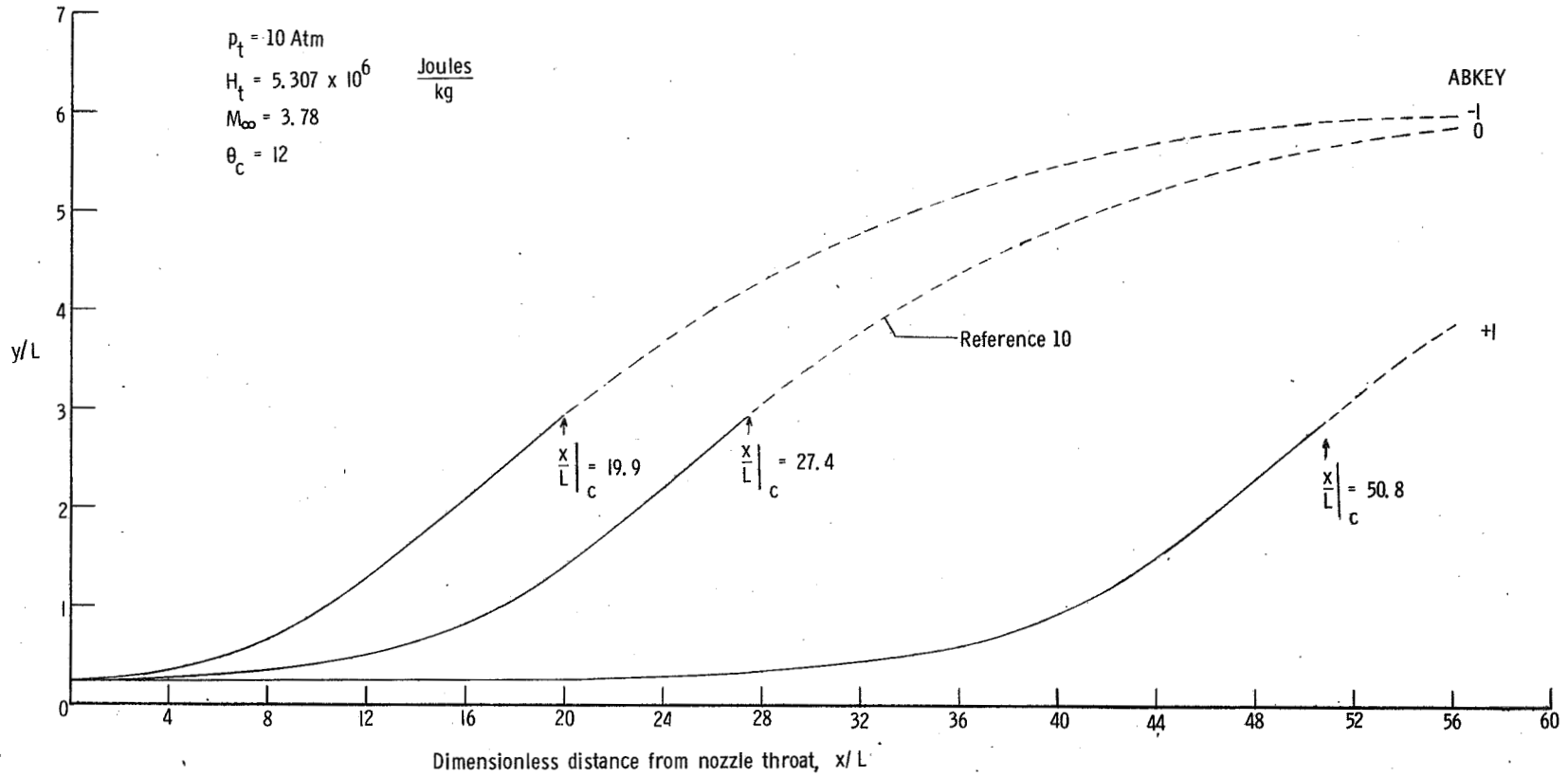


Figure 3.- The effect of three different center-line Mach number distributions in the expansion region of a real-gas two-dimensional nozzle contour ($\gamma \approx 1.25$).

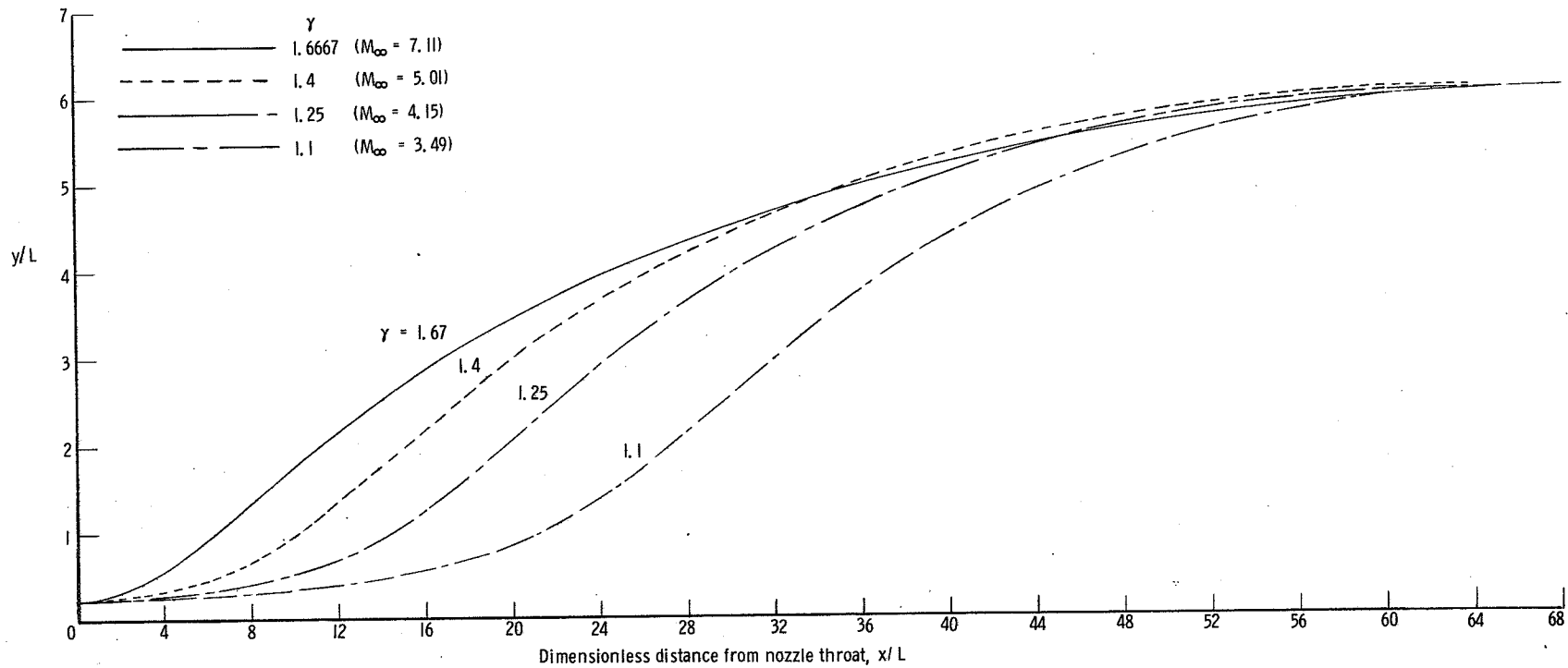


Figure 4.- The effect of gamma on two-dimensional nozzle contours with a constant throat-to-exit area ratio ($\theta_c = 12^\circ$, ABKEY = 0).

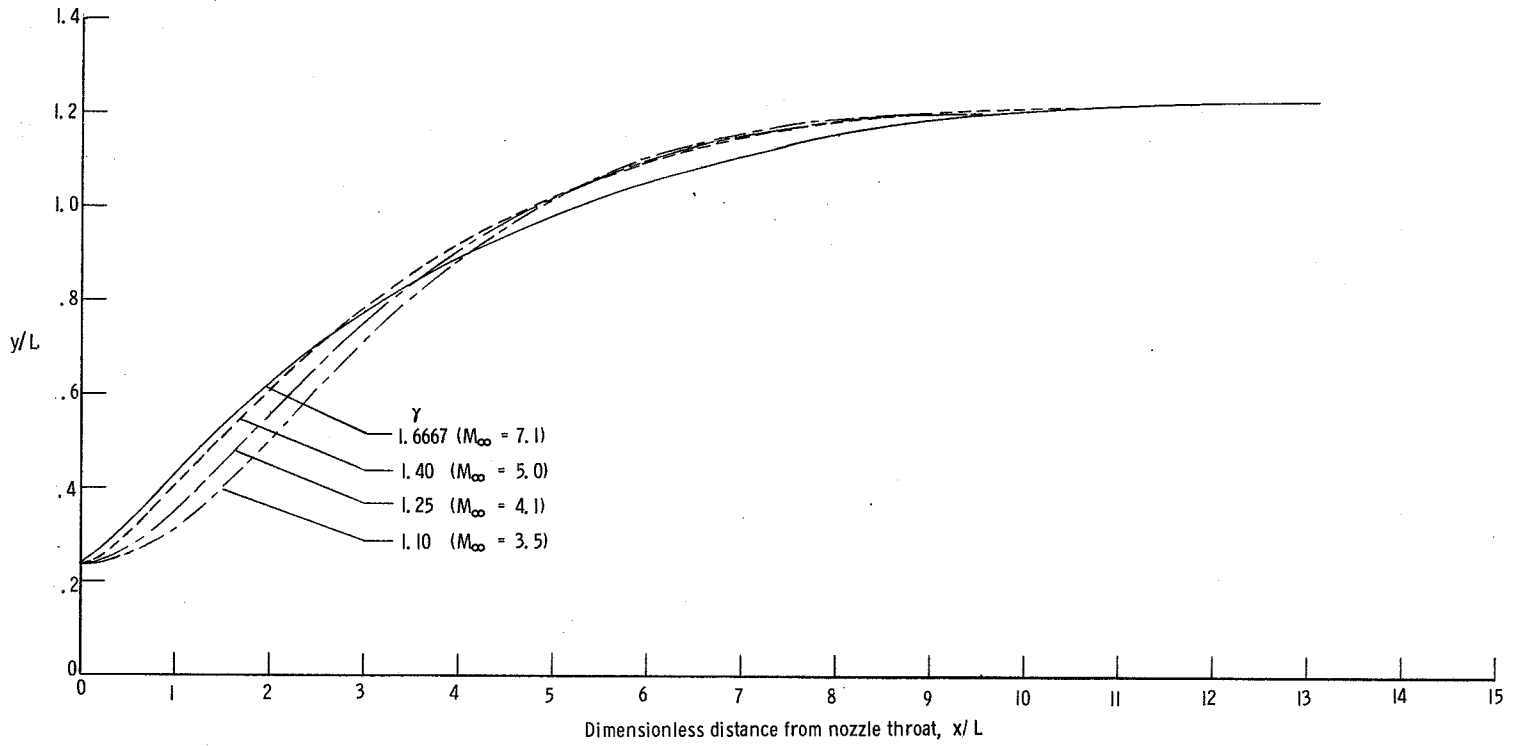


Figure 5.- The effect of gamma on axisymmetric nozzle contours with a constant throat-to-exit area ratio.

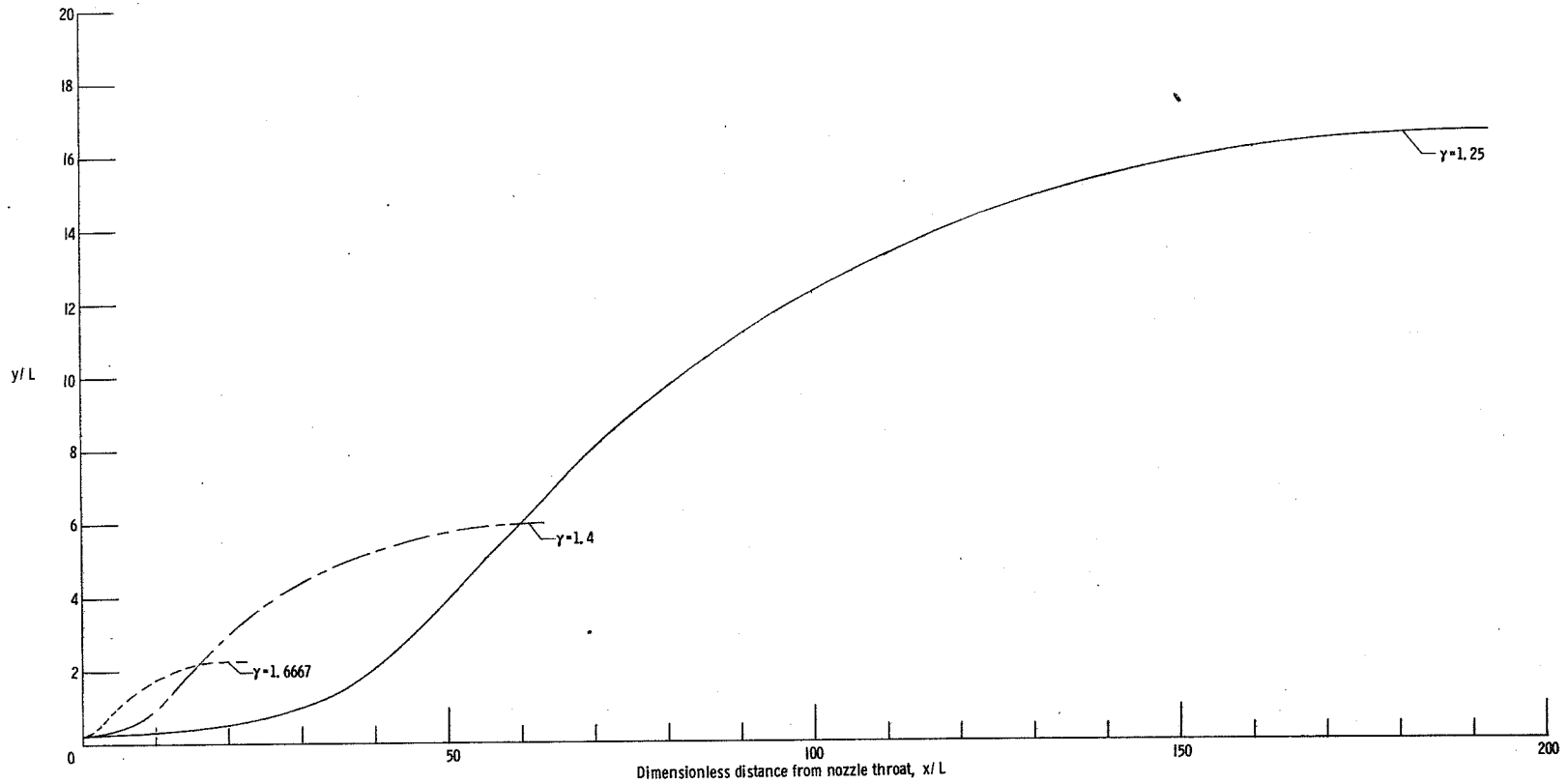


Figure 6.- The effect of gamma on two-dimensional nozzle contours with a constant exit Mach number of 5.0
 $(\theta_c = 12^\circ, ABKEY = 0)$.

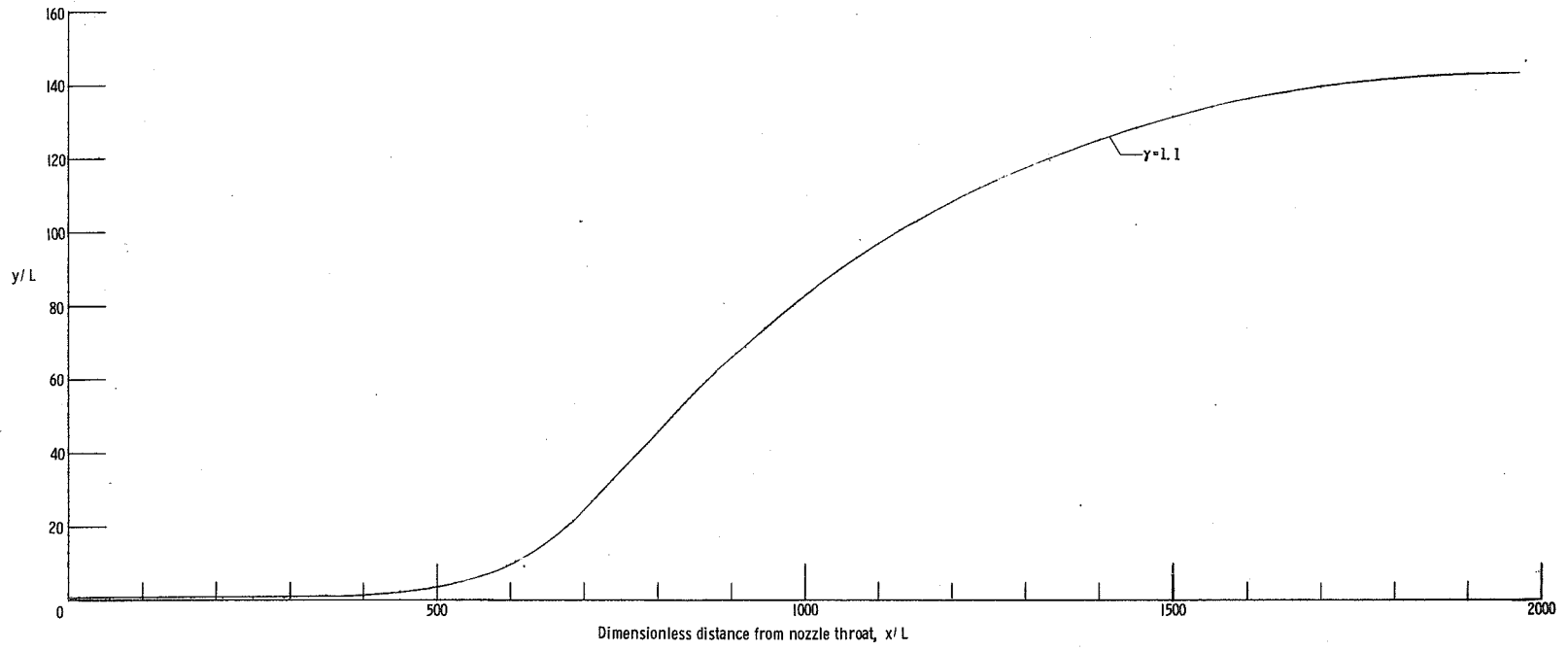


Figure 6.- Concluded.

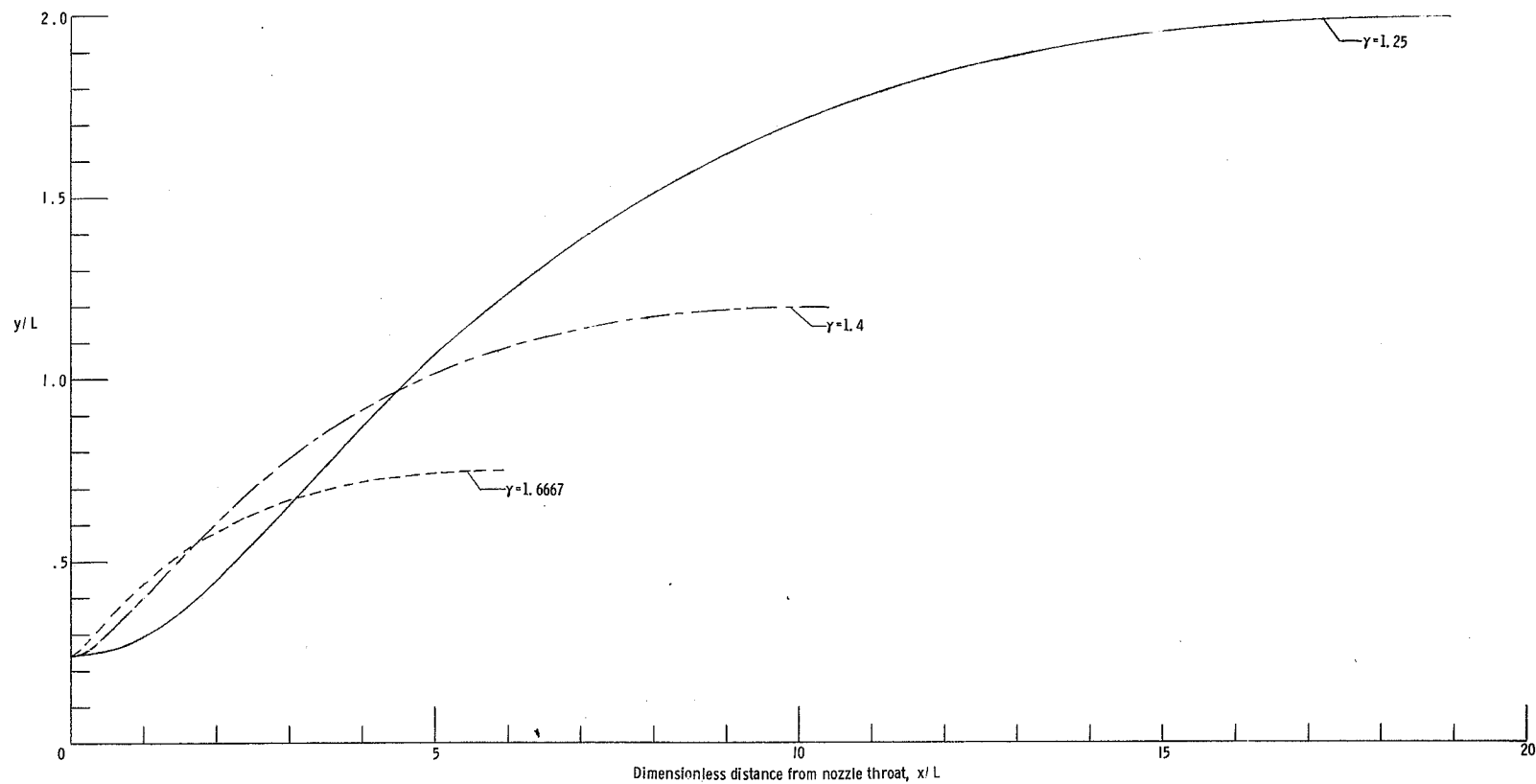


Figure 7.- The effect of gamma on axisymmetric nozzle contours with a constant exit Mach number of 5.0 ($\theta_c = 12^\circ$, ABKEY = 0).

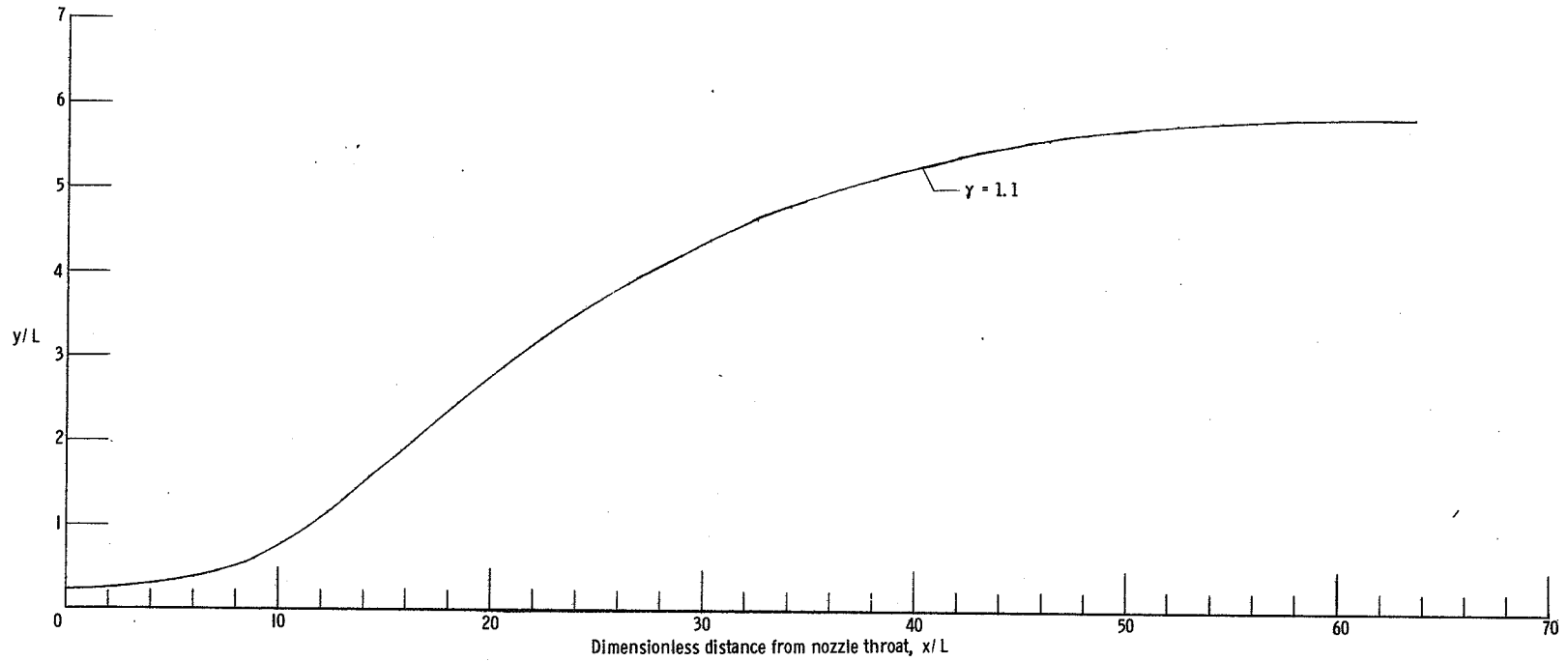


Figure 7.- Concluded.

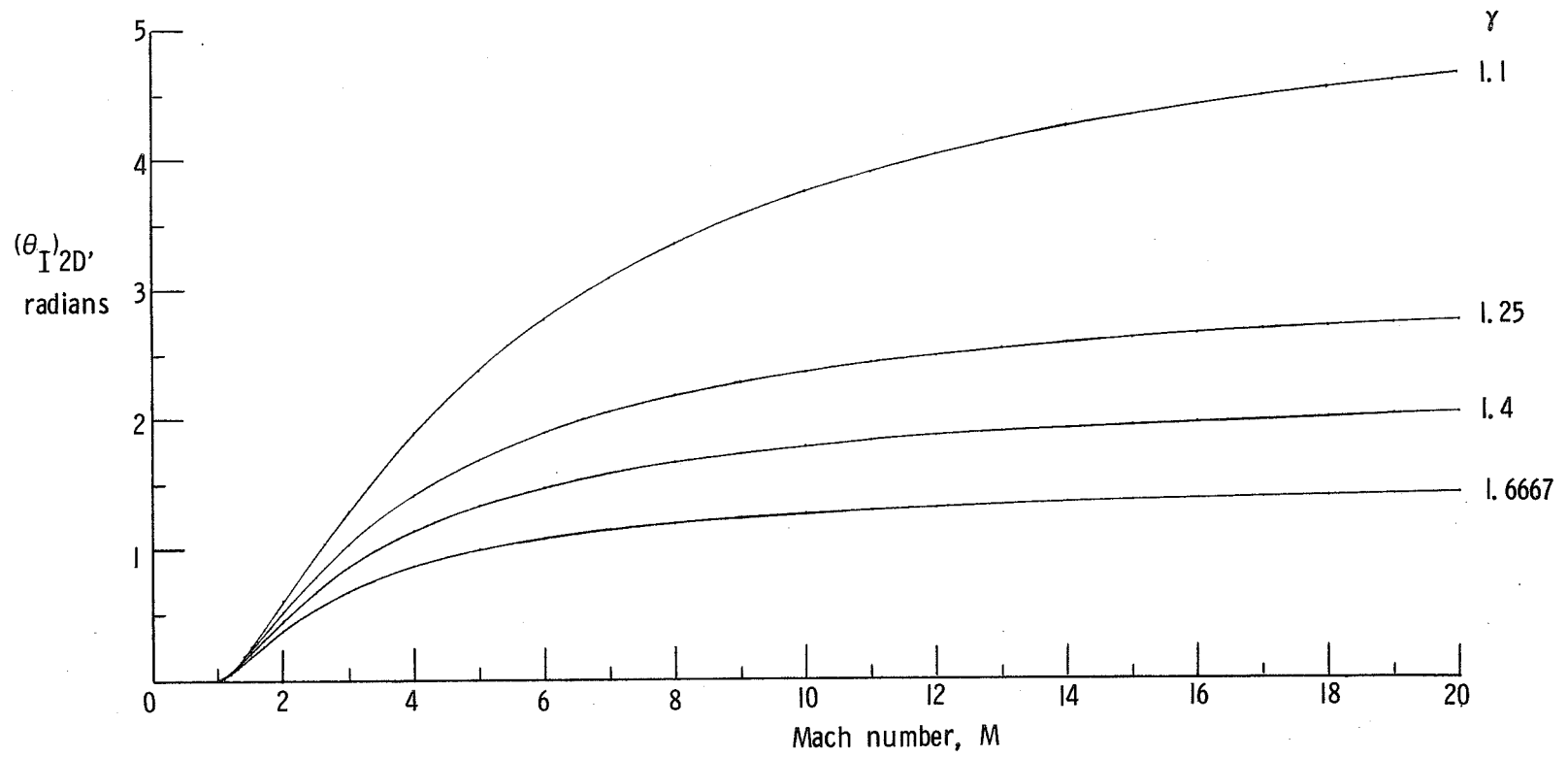


Figure 8.- The integrated flow angle as a function of Mach number for two-dimensional flow and various ratios of specific heats.

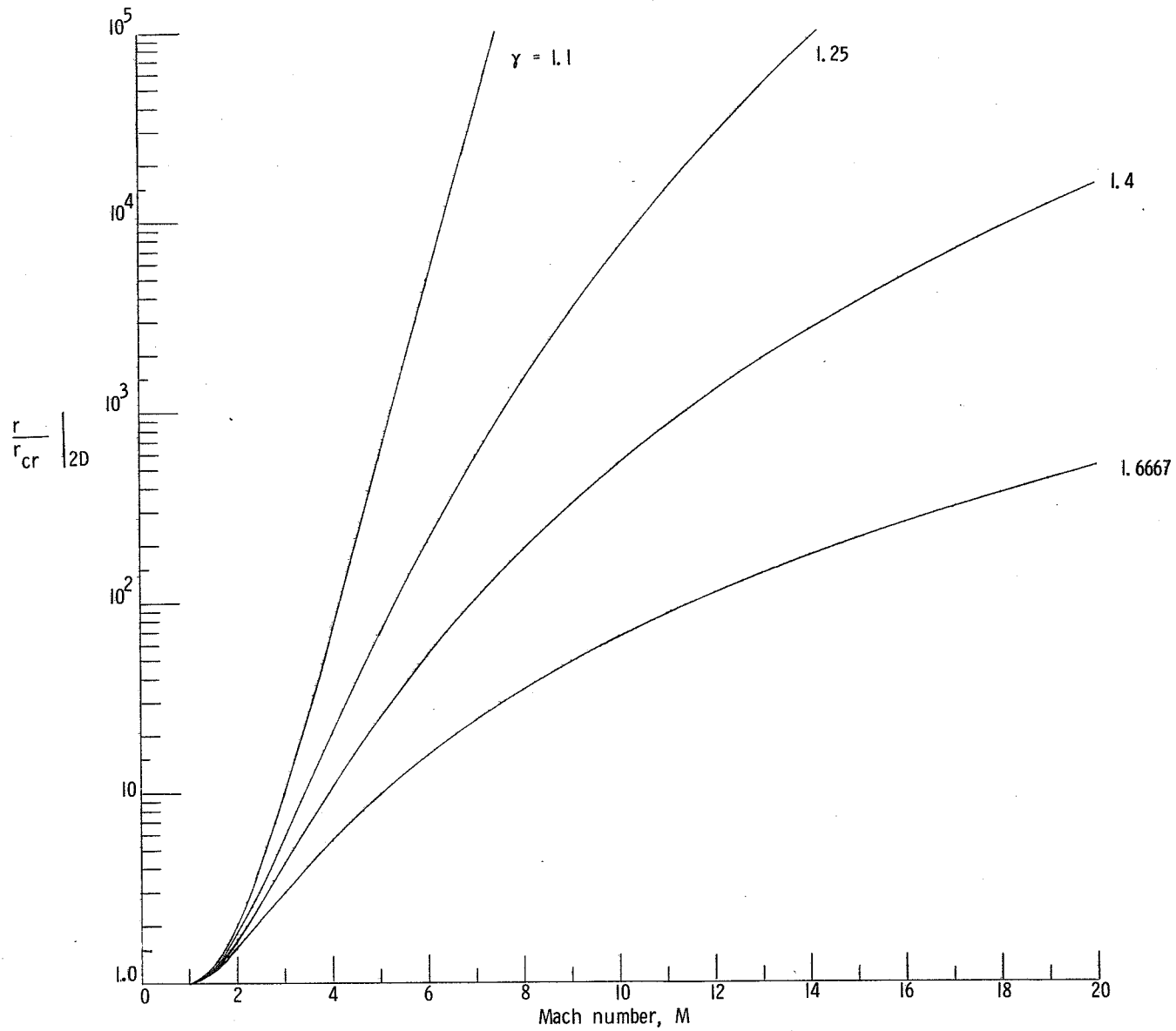


Figure 9.- The dimensionless radial-flow coordinate for two-dimensional flow as a function of Mach number for various ratios of specific heats.

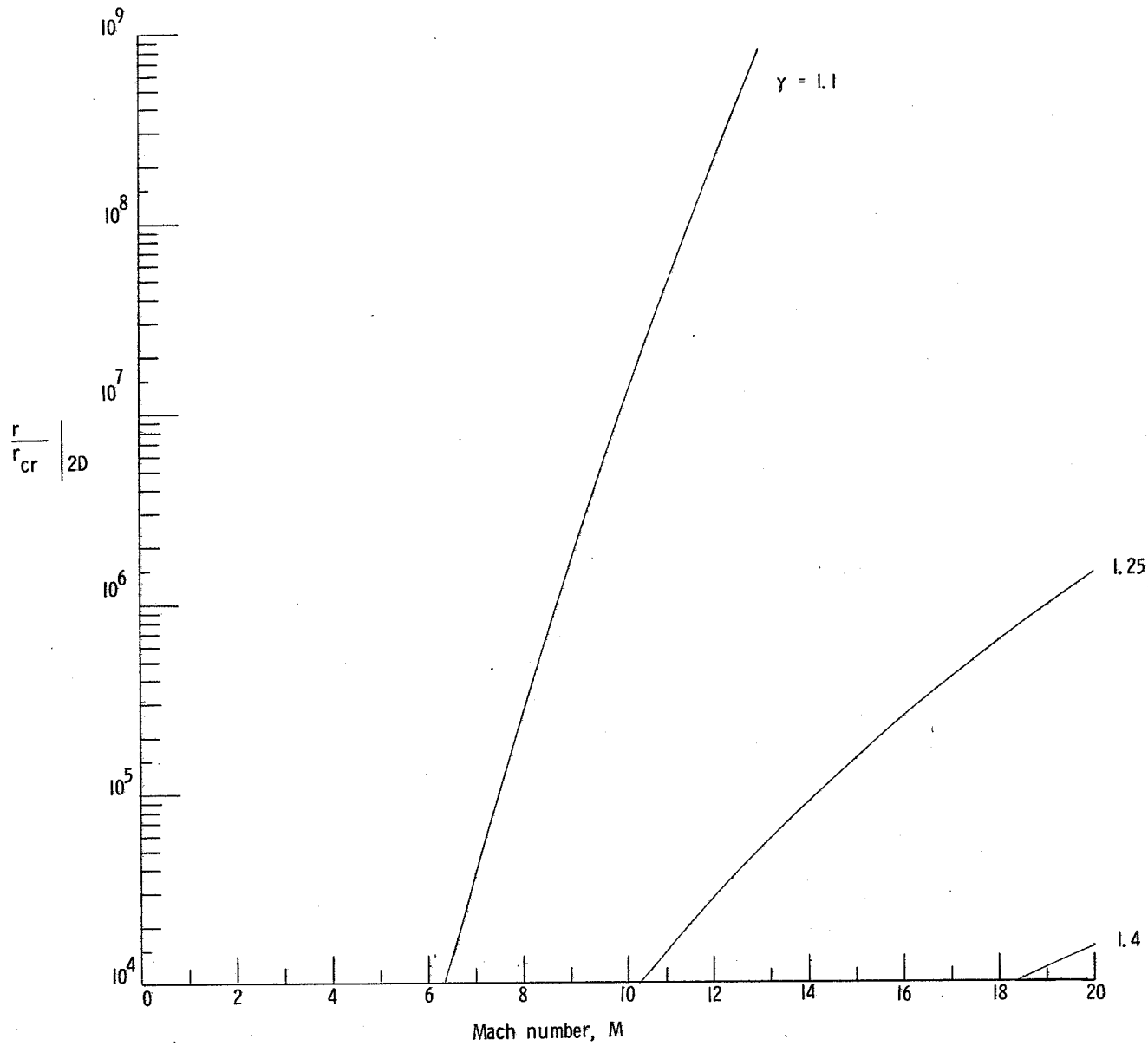


Figure 9.- Continued.

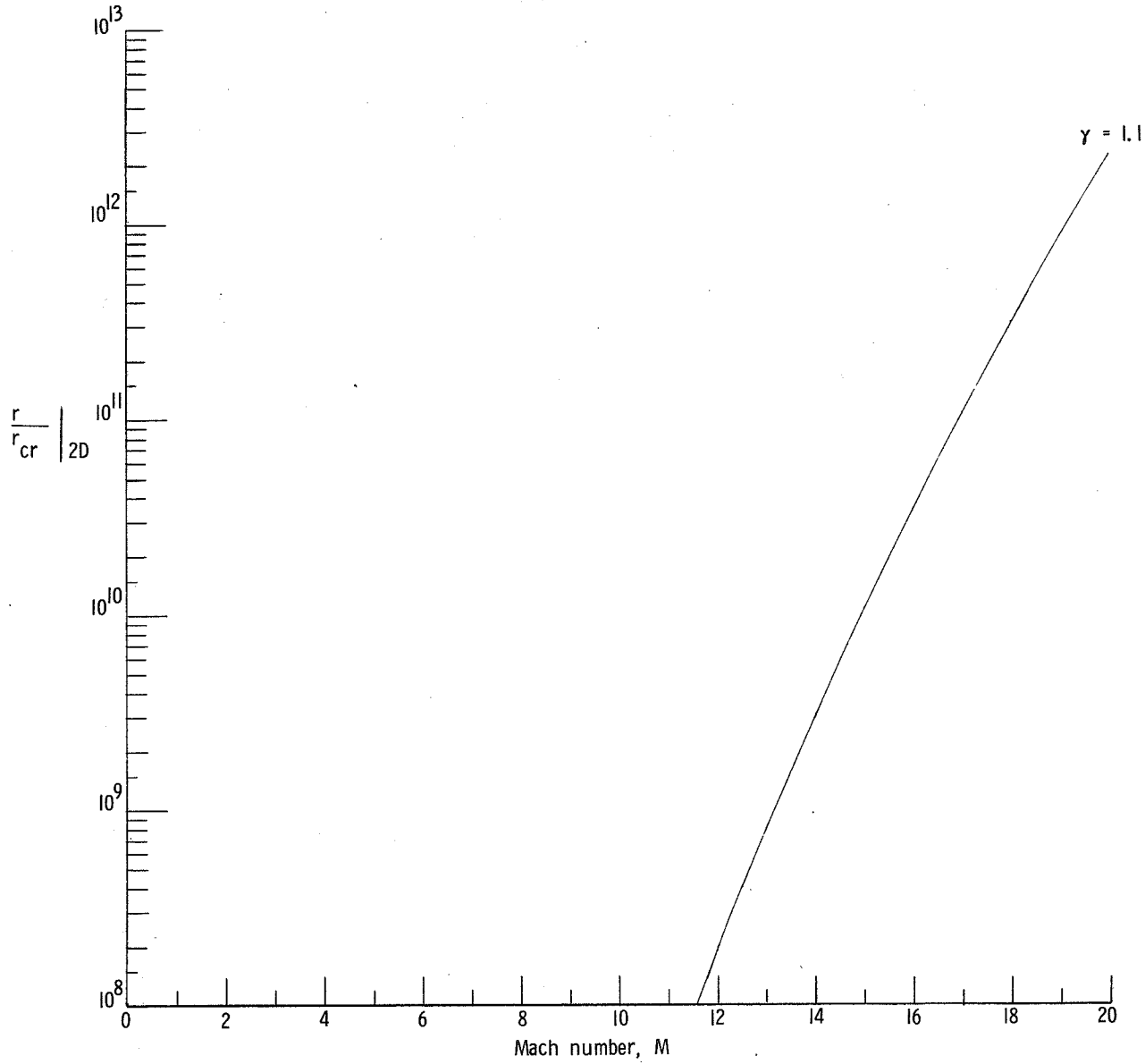


Figure 9.- Concluded.

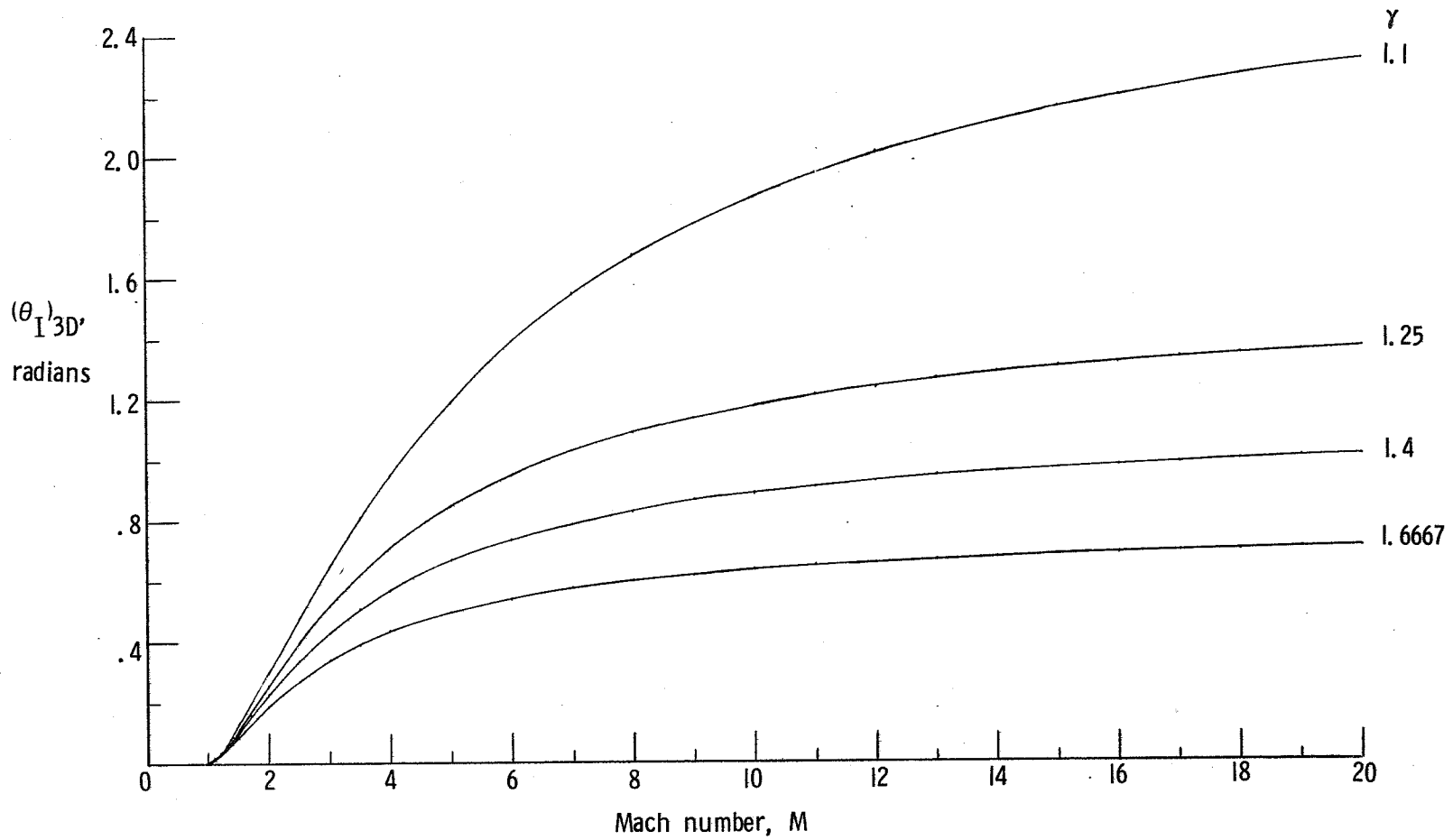


Figure 10.- The integrated flow angle as a function of Mach number for axisymmetric flow and various ratios of specific heats.

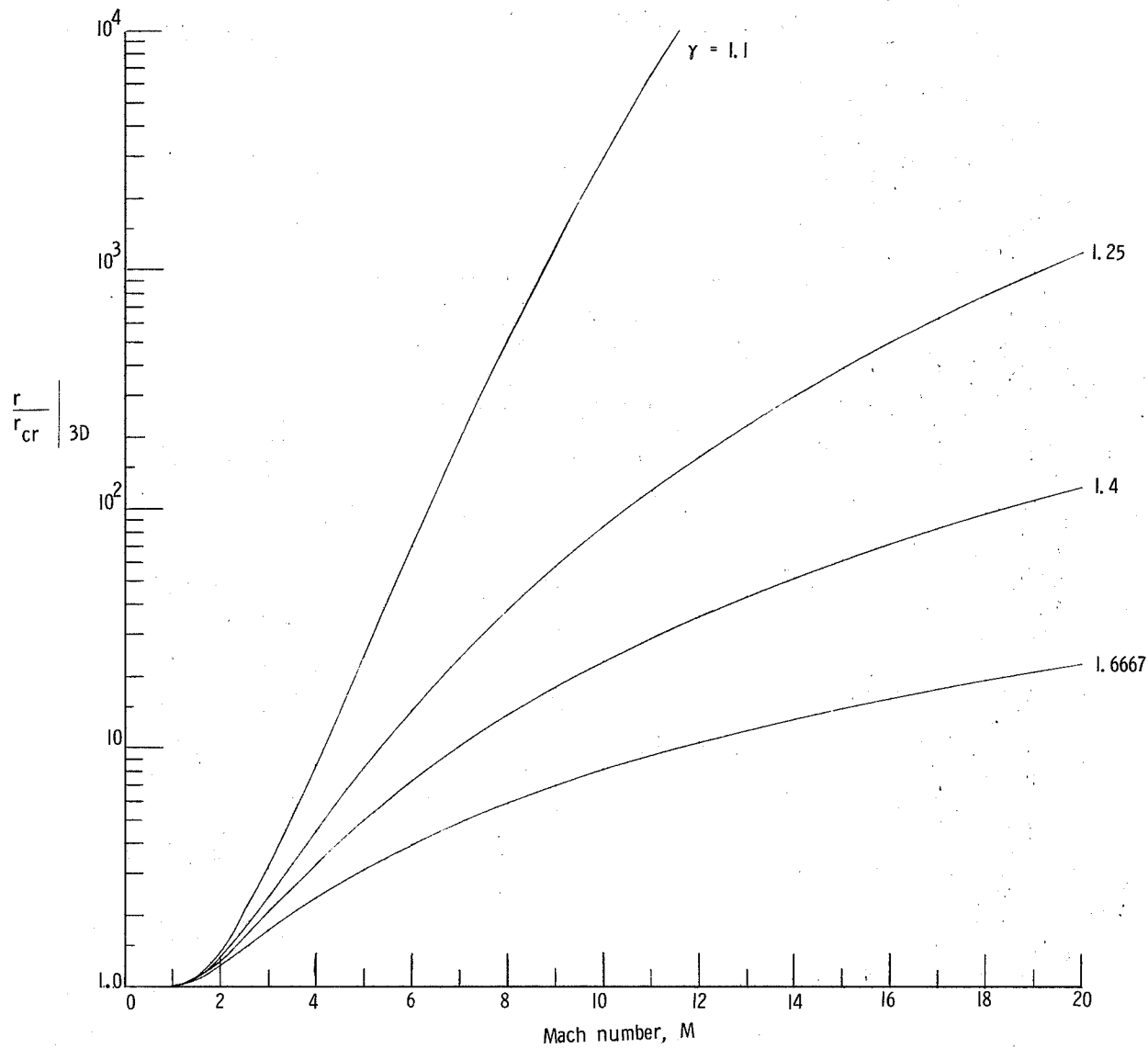


Figure 11.- The dimensionless radial-flow coordinate for axisymmetric flow as a function of Mach number for various ratios of specific heats.

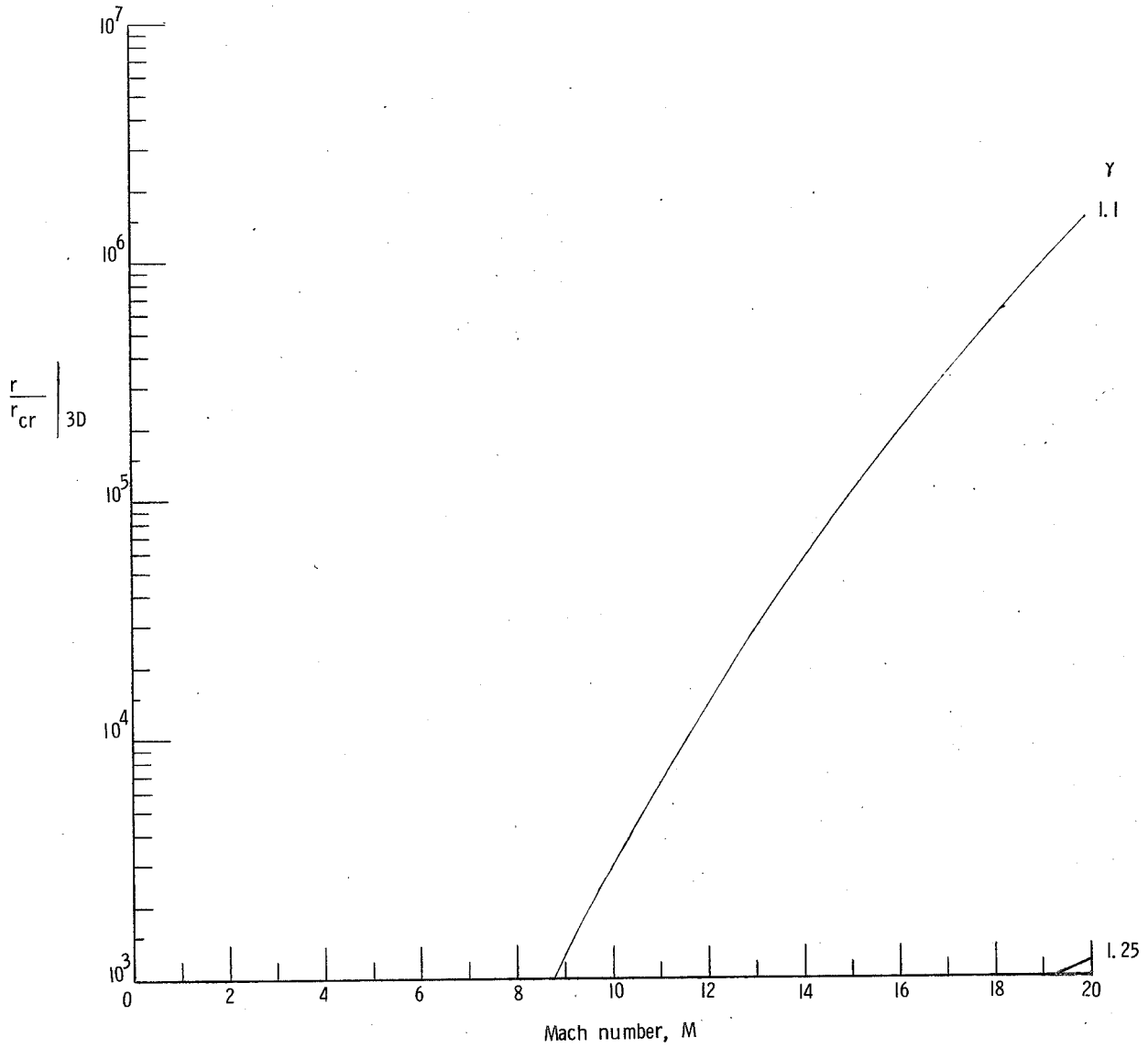


Figure 11.- Concluded.

1. Report No. NASA TM X-3243		2. Government Accession No.		3. Recipient's Catalog No.	
4. Title and Subtitle A METHOD FOR CALCULATING A REAL-GAS TWO-DIMENSIONAL NOZZLE CONTOUR INCLUDING THE EFFECTS OF GAMMA				5. Report Date September 1975	
				6. Performing Organization Code	
7. Author(s) Charles B. Johnson and Lillian R. Boney				8. Performing Organization Report No. L-10144	
9. Performing Organization Name and Address NASA Langley Research Center Hampton, Va. 23665				10. Work Unit No. 505-11-31-02	
				11. Contract or Grant No.	
12. Sponsoring Agency Name and Address National Aeronautics and Space Administration Washington, D.C. 20546				13. Type of Report and Period Covered Technical Memorandum	
				14. Sponsoring Agency Code	
15. Supplementary Notes					
16. Abstract <p>A method for calculating two-dimensional inviscid nozzle contours for a real gas or an ideal gas by the method of characteristics is described. The method consists of a modification of an existing nozzle computer program. The ideal-gas nozzle contour can be calculated for any constant value of gamma. Two new methods of calculating the center-line boundary values of the Mach number in the throat region are also presented. The use of these three methods of calculating the center-line Mach number distribution in the throat region can change the distance from the throat to the inflection point by a factor of 2.5.</p> <p>The effect of ratios of specific heat (gamma) equal to 1.6667, 1.4, 1.25, and 1.1 on two-dimensional nozzle contours with constant area ratios and nearly constant lengths showed that a decrease in gamma resulted in a much more gradual opening of the nozzle contour from the throat into the expansion region. For similar area ratio and length constraints and for the same values of gamma, calculations of axisymmetric nozzle contours showed a trend similar to that of the two-dimensional nozzle contours; however, the effect of gamma on the axisymmetric contours was not nearly as pronounced as the effect on the two-dimensional contours. The effect of gammas of 1.6667, 1.4, 1.25, and 1.1 was investigated for two-dimensional and axisymmetric inviscid nozzle contours with a constant exit Mach number. The effect of decreasing the gamma in the calculation of the two-dimensional nozzle contour resulted in a more gradual opening of the nozzle from the throat into the expansion region. The effect on axisymmetric contours for calculations made with the same four values of gamma was similar to the effect found for the two-dimensional contours; however, the effect on the axisymmetric contours was not as pronounced as the effect on the two-dimensional contours. For the two-dimensional nozzle, contours with a constant exit Mach number, the ratio of the exit height to throat height increased sharply with a decrease in the value of gamma. For a fixed throat size, the length of the two-dimensional nozzle decreased significantly with an increase in the value of gamma.</p> <p>A user's guide is presented for input to the computer program for both the two-dimensional and axisymmetric nozzle contours.</p>					
17. Key Words (Suggested by Author(s)) Nozzle contour Method of characteristic Effects of ratios of specific heat			18. Distribution Statement Unclassified - Unlimited Subject Category 34		
19. Security Classif. (of this report) Unclassified		20. Security Classif. (of this page) Unclassified		21. No. of Pages 39	22. Price* \$3.75